JOURNAL OF PETROLOGY | VOLUME 39 | NUMBER 7 | PAGES 1285–1306 | 1998

Tracing the Indian Ocean Mantle Domain Through Time: Isotopic Results from Old West Indian, East Tethyan, and South Pacific Seafloor

J. J. MAHONEY[1]*, R. FREI[2], M. L. G. TEJADA[1], X. X. MO[3], P. T. LEAT[4] AND T. F. NÄGLER[5]

[1]SCHOOL OF OCEAN AND EARTH SCIENCE AND TECHNOLOGY, UNIVERSITY OF HAWAII, HONOLULU, HI 96822, USA

[2]GEOLOGISK INSTITUT, KOBENHAVNS UNIVERSITET, KOBENHAVN, DENMARK

[3]GRADUATE SCHOOL, CHINA UNIVERSITY OF GEOSCIENCES, BEIJING 100 083, CHINA

[4]BRITISH ANTARCTIC SURVEY, HIGH CROSS, MADINGLEY ROAD, CAMBRIDGE CB3 0ET, UK

[5]MINERALOGISCH-PETROGRAPHISCHES INSTITUT, UNIVERSITÄT BERN, ERLACHSTR. 9A, CH-3012 BERN, SWITZERLAND

RECEIVED JUNE 9, 1997; REVISED TYPESCRIPT ACCEPTED FEBRUARY 3, 1998

The isotopic difference between modern Indian Ocean and Pacific or North Atlantic Ocean ridge mantle (e.g. variably lower $^{206}Pb/^{204}Pb$ for a given ε_{Nd} and $^{208}Pb/^{204}Pb$) could reflect processes that occurred within a few tens of millions of years preceding the initial breakup of Gondwana. Alternatively, the Indian Ocean isotopic signature could be a much more ancient upper-mantle feature inherited from the asthenosphere of the eastern Tethyan Ocean, which formerly occupied much of the present Indian Ocean region. Age-corrected Nd, Pb, and Sr isotopic data for 46–150 Ma seafloor lavas from sites in the western Indian Ocean and ocean-ridge-type Tethyan ophiolites (Masirah, Yarlung–Zangpo) reveal the presence of both Indian-Ocean-type compositions and essentially Pacific–North Atlantic-type signatures. In comparison, Jurassic South Pacific ridge basalts from Alexander Island, Antarctica, possess normal Pacific–North Atlantic-type isotopic ratios. Despite the very sparse sampling of old seafloor, the age-corrected $\varepsilon_{Nd}(t)$ values of the old Indian Ocean basalts cover a greater range than seen for the much more thoroughly sampled present-day spreading axes and islands within the Indian Ocean (e.g. 18 ε_{Nd} units for basalts in the 60–80 Ma range vs 15 ε_{Nd} units for 0–10 Ma ones). The implications of these results are that the upper mantle in the Indian Ocean region is becoming increasingly well mixed through time, and that the Indian Ocean mantle domain may not greatly pre-date the age of earliest spreading in the Indian Ocean.

KEY WORDS: *mantle geochemistry; old Indian Ocean; Tethyan crust*

INTRODUCTION

Isotopic studies of MORB (mid-ocean ridge basalts) have established the existence of a vast mantle domain in the Indian Ocean distinct from the sources of Pacific and North Atlantic MORB. Along the present Indian Ocean spreading axes, this domain includes the entire Central Indian and Carlsberg ridges and most of the Southeast and Southwest Indian ridges, stretching from about 126°E on the Southeast Indian Ridge (Klein *et al.*, 1988; Pyle *et al.*, 1992) to about 26°E on the Southwest Indian Ridge (Mahoney *et al.*, 1992) and northward into the Red Sea (e.g. Schilling *et al.*, 1992; Volker *et al.*, 1993). Indian MORB are characterized, in particular, by lower

*Corresponding author. Telephone: 808-956-8705. e-mail: jmahoney@soest.hawaii.edu

values of $^{206}Pb/^{204}Pb$ relative to ε_{Nd} and $^{208}Pb/^{204}Pb$ than Pacific and North Atlantic MORB, and also tend to have comparatively high $^{87}Sr/^{86}Sr$ (e.g. Hedge *et al.*, 1979; Dupré & Allègre, 1983; Hamelin *et al.*, 1986; Michard *et al.*, 1986; Price *et al.*, 1986; Dosso *et al.*, 1988; Mahoney *et al.*, 1989, 1992; Hall *et al.*, 1995). When isotopic data for samples from the fringes of the Indian Ocean domain are removed from consideration, there is remarkably little overlap of the Indian MORB data set with the isotopic field defined by >95% of published Pacific and North Atlantic MORB data in either the ε_{Nd} vs $^{206}Pb/^{204}Pb$ or $^{208}Pb/^{204}Pb$ vs $^{206}Pb/^{204}Pb$ diagrams (Fig. 1). Furthermore, recent studies of Western Pacific back-arc and marginal basin lavas (e.g. Hochstaedter *et al.*, 1990; Loock *et al.*, 1990; Hickey-Vargas, 1991, 1998; Tu *et al.*, 1992; Crawford *et al.*, 1995; Hickey-Vargas *et al.*, 1995; Spadea *et al.*, 1996), and of island-arc lavas in the Philippines (Mukasa *et al.*, 1987; Castillo, 1996), show that isotopically Indian-MORB-like asthenosphere also underlies this region and thus appears to extend far to the east of the Indian Ocean proper. However, despite its great size, the history and origins of this domain (i.e. why it is different from Pacific and North-Atlantic-type mantle) are understood only poorly.

Two general classes of hypotheses have been proposed to account for the Indian Ocean asthenospheric domain. One is that it was created shortly before and during the breakup of Gondwana in the processes that formed the Indian Ocean itself. Possible causes involve either upwelling of deep, isotopically unusual plume-related mantle or widespread introduction of small amounts of continental lithospheric or old, shallowly subducted sedimentary material into the MORB source mantle (promoted by Gondwanan rifting, subduction–erosion, and/or the erosive action of the Kerguelen, Marion, Crozet, and Bouvet starting-plume heads) (e.g. Castillo, 1988; Klein *et al.*, 1988; le Roex *et al.*, 1989; Mahoney *et al.*, 1989, 1992; Storey *et al.*, 1989, 1992; Pyle *et al.*, 1992, 1995; Weis *et al.*, 1992; Hickey-Vargas *et al.*, 1995; Rehkämper & Hofmann, 1997). In either case, this material is postulated to have been dispersed to its present extent along asthenospheric flow paths as the Indian Ocean opened. In this class of hypotheses, older Indian MORB would be expected to show more variable isotopic signatures than modern ones because less time would have been available for intermixing of 'normal' (i.e. Pacific–North Atlantic type) and contaminated asthenosphere. Depending upon their location and age, and the nature of asthenospheric dispersal patterns, some older lavas might not have Indian-MORB-type isotopic signatures at all; the same would probably be true of seafloor formed north of Greater India in the eastern Tethyan Ocean (Mahoney *et al.*, 1992), the Mesozoic ocean that existed in much of the same region now occupied by the Indian Ocean before opening of the latter. An alternative

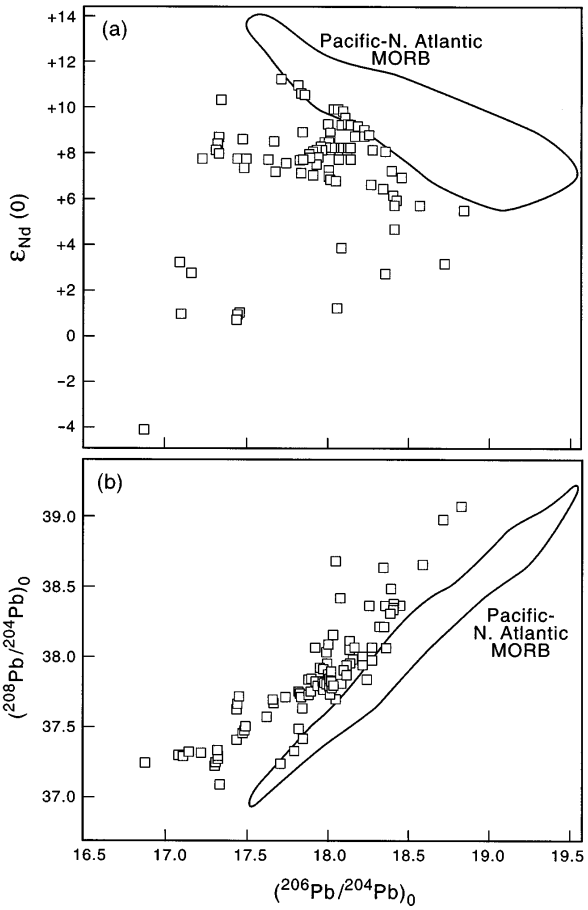

Fig. 1. Plot of ε_{Nd} (a) and $^{208}Pb/^{204}Pb$ (b) vs $^{206}Pb/^{204}Pb$ for Indian MORB (□) compared with the field defined by >95% of published high-quality data for Pacific and North Atlantic MORB. Data for the edges of the modern Indian Ocean mantle domain, where some transitional compositions occur, are excluded (i.e. in the Australian–Antarctic Discordance, along the western Southwest Indian Ridge, and Red Sea–Gulf of Aden). Principal MORB data sources include those cited in the text, plus Ito *et al.* (1987), White *et al.* (1987), Hanan & Schilling (1989), Dosso *et al.* (1993), Bach *et al.* (1994), Mahoney *et al.* (1994), and other recent studies cited therein.

hypothesis is that the Indian MORB mantle domain is a much longer-lived asthenospheric feature that existed well before the Indian Ocean started opening up (e.g. Hart, 1984; Crawford *et al.*, 1995). In this case, the characteristic Indian-Ocean-type isotopic signature would be expected to be typical of both old Indian MORB and seafloor erupted in a widespread region of the Tethyan Ocean.

Recently, Lanyon (1995), Pyle *et al.* (1995), and Weis & Frey (1996) have studied old seafloor basalts from drill and dredge sites in the eastern Indian Ocean east of about 90°E. Their results indicate that lavas with ages ranging from 15 to 125 Ma exhibit rather typical Indian-MORB-type isotopic signatures; that is, values lying to

the low-$^{206}Pb/^{204}Pb$ side of the Pacific–North Atlantic MORB fields in Fig. 1. However, ~150 Ma samples from Deep Sea Drilling Project Site 261 (off the northwestern corner of Australia) lack clear Indian-MORB-type characteristics, and the same may be true of similar-age MORB from nearby Site 765 (see Weis & Frey, 1996). Although preserved within the northeastern corner of the Indian Ocean, these basalts were formed around 30–35°S at a Tethyan spreading center some 15 my before significant spreading began in the eastern Indian Ocean between Greater Indo-Madagascar and Australia–Antarctica (e.g. Ogg *et al.*, 1992).

In this paper, we present results for 46–140 Ma lavas from drill sites in the western Indian Ocean. Also, although the eastern Tethyan Ocean no longer exists, fragments of Tethyan seafloor are preserved in MORB-type ophiolites along the Tethyan suture belt in southern Asia (Fig. 2). Here, we discuss results for two such suites: 110 Ma basalts from the Yarlung–Zangpo suture of Tibet, and a group of 150 Ma and 120 Ma rocks from the Masirah ophiolite off the Arabian peninsula. As a comparison, we also present isotopic data for Jurassic Pacific MORB from Alexander Island, Antarctica.

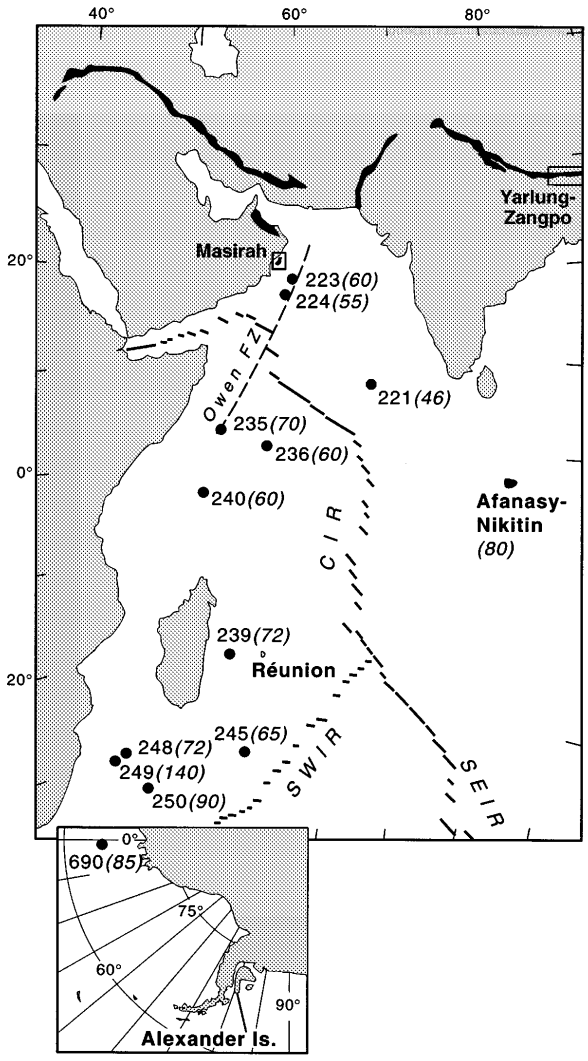

Fig. 2. Map of the western Indian Ocean showing locations of the drill sites (with basement ages or age estimates in parentheses), Masirah, and Yarlung–Zangpo basalts. The belt of Tethyan ophiolites and colored mélanges in southern Asia is depicted in black (after Coleman, 1981). Inset shows locations of Site 690 and Alexander Island. CIR, Central Indian Ridge; SWIR, Southwest Indian Ridge; SEIR, Southeast Indian Ridge. It should be noted that the large difference in age between Site 249 and nearby Site 248 reflects a major boundary in seafloor age provinces (e.g. Simpson *et al.*, 1974).

METHODS

Several of the samples studied were fairly fresh but most were affected by seawater-mediated alteration, ranging from mild 'brownschist' to zeolite, prehnite–pumpellyite or, in some cases, lower greenschist facies (see Davies *et al.*, 1974; Fisher *et al.*, 1974; Simpson *et al.*, 1974; Whitmarsh *et al.*, 1974; Moseley & Abbotts, 1979; Abbotts, 1981; Girardeau *et al.*, 1985; Pearce & Deng, 1988; Doubleday *et al.*, 1994). Rarely, we were able to pick enough fresh glass or clear-looking plagioclase for isotopic and isotope-dilution analysis; glass and plagioclase separates were cleaned ultrasonically in ultrapure, 1 M HCl and water before dissolution and further processing. For other samples, we followed a preparation procedure closely similar to that used in our previous isotopic studies of old, non-glassy submarine basalts. Chips from the least-altered interior portions of samples were broken to pieces of 3–5 mm in size, which were handpicked under a microscope to avoid visible alteration products (veins, vesicle fillings, and more altered patches of groundmass). The pieces selected were briefly cleaned ultrasonically in ultrapure, weak HF–HNO_3 and H_2O (in sequence) and then broken into smaller (~2 mm) pieces, after which the picking and cleaning procedure was repeated. The pieces chosen were ground in a boron carbide mortar, dissolved, and analyzed for isotopic ratios of Nd, Pb, and Sr and isotope-dilution abundances of Nd, Sm, Pb, Th, U, Sr, and Rb at the University of Hawaii. Several of the samples from Masirah (those lacking MSX or MA prefixes in the tables) were analyzed for Nd and Pb isotopes and Nd, Sm, Pb, and U abundances at the University of Bern following a generally similar preparation procedure; Th was analyzed for these samples at the University of Hawaii. In addition, isotopic ratios and parent–daughter element abundances were determined for some samples on splits of powder subjected to a multistep, HCl-dominated acid-leaching procedure effective at removing low-temperature alteration phases (carbonates, clays, chlorite, phosphate, zeolites, ferromanganese oxides; some fresh material is also removed

in the process; see Mahoney, 1987; Mahoney & Spencer, 1991). It should be noted that because the picking procedure, as well as acid leaching, when employed, variably modifies a sample's mineralogical composition relative to that of the bulk rock, the isotope-dilution data do not strictly represent bulk-rock elemental abundances and are used here for isotopic age-corrections only. The results are given in Tables 1 and 2.

Very few trace element data have been published for the western Indian Ocean drillhole lavas. Thus, we analyzed a subset of the bulk-rock samples for a broad suite of trace elements; we also analyzed several Masirah samples. Slabs of fresher portions of rock with a minimum of veins and amygdules were chosen (note that for some of the smaller drillhole samples, the freshest looking material had already been reserved for isotopic work). To avoid possible drilling- and/or handling-related contamination, the slabs (typically 5–30 cm^3) were taken from sample interiors, lapped with SiC, cleaned briefly (~5 min) in ultrapure, weak HF–HNO_3 (each ~0·2 M) and water in an ultrasonic bath and powdered in alumina; experience has shown that this procedure does not significantly modify bulk-basalt compositions for the elements analyzed. The resulting bulk-rock powders were prepared and analyzed by inductively coupled plasma-mass spectrometry at the University of Hawaii following techniques similar to those described by Jain & Neal (1996). The data appear in Table 3.

A note on effects of alteration on isotopic ratios

Because seawater has a fairly high concentration of Sr (~8 ppm; e.g. Li, 1991) and high $^{87}Sr/^{86}Sr$ (today ~0·709) relative to oceanic mantle, $^{87}Sr/^{86}Sr$ values in basalts altered by seawater-derived solutions are typically elevated above values in pristine samples; in constrast, Nd and Sm abundances are extremely low in seawater (4×10^{-6} and 8×10^{-7} ppm, respectively) and Nd isotopes are resistant to modification by even rather high amounts of alteration (e.g. McCulloch *et al.*, 1981; Staudigel *et al.*, 1995). Like Nd, Pb abundances in seawater are very low (2×10^{-6} ppm), so that Pb isotope ratios are affected little by seawater interaction. Pb can be mobile in hydrothermal systems, but redeposition of Pb from one part of a volcanic system to another will normally not be isotopically distinguishable (unless the system possesses significant local-scale isotopic heterogeneity). However, unlike $^{147}Sm/^{144}Nd$ values, $^{238}U/^{204}Pb$ ratios (and to a lesser extent, $^{232}Th/^{204}Pb$) can be affected markedly by mobility of U and uptake of U from seawater ($3·2 \times 10^{-3}$ ppm), in particular, as well as Pb (and sometimes Th) mobility (e.g. Tatsumoto, 1978; Macdougall *et al.*, 1979; Chen & Pallister, 1981). If alteration of an oceanic basalt occurs within several million years after eruption, as typically appears to be the case (e.g. Staudigel *et al.*, 1981), and the rock remains a nearly closed system thereafter, then age-correction of Pb isotope ratios will result in values close to the initial magmatic values even for an old specimen. Indeed, previous studies have demonstrated that good initial-Pb isotope information can be obtained on a range of crystalline magmatic rocks with hydrothermal overprints as high as greenschist facies (e.g. Chen & Pallister, 1981; Göpel *et al.*, 1984). However, if alteration of parent–daughter ratios occurs long after eruption, or repeatedly over many millions of years, then age-adjusted Pb isotopic values will be erroneous. As a hypothetical illustration, let us consider a basalt erupted at 100 Ma whose $^{238}U/^{204}Pb$ ratio has been elevated from an original value of, say, 10 to 40 by some very recent seawater-alteration process; using the measured value of 40 to calculate an 'initial' $^{206}Pb/^{204}Pb$ ratio leads to a substantial overcorrection of 0·47.

RESULTS

Old Pacific MORB

The basalts of Alexander Island represent faulted slices of Jurassic seafloor formed by spreading between the Pacific and Phoenix plates, and preserved in an accretionary wedge complex (Doubleday *et al.*, 1994). Ages are well determined at 150 Ma in one location (Sullivan Glacier; samples KG 3513-27 and KG 3513-4) and relatively poorly known at a second (Herschel Heights), where a 150 Ma age is assumed; a third area (Lully Foothills) is well dated at Early Jurassic (~200 Ma). Chemically, the basalts include both normal-type and incompatible-element-enriched MORB (N- and E-MORB); ocean-island-type compositions are also present (Doubleday *et al.*, 1994). The samples we analyzed isotopically are altered to zeolite and prehnite–pumpellyite facies.

In an initial $\varepsilon_{Nd}(t)$ vs $(^{87}Sr/^{86}Sr)_t$ diagram (Fig. 3), most of the Alexander Island data lie to the high-$^{87}Sr/^{86}Sr$ side of the MORB field: although $\varepsilon_{Nd}(t)$ is between $+8·6$ and $+5·4$, within the range of modern N- and E-MORB, the $(^{87}Sr/^{86}Sr)_t$ of unleached splits varies from 0·70295 to 0·70439. In contrast to many of the drillhole and Masirah samples (see below), acid-leaching of the two Alexander Island samples whose unleached splits had the highest age-adjusted Sr isotope ratios produced only modest decreases in $(^{87}Sr/^{86}Sr)_t$, not enough to move their data points into the MORB field in Fig. 3. This result probably reflects the fact that the main repository of Sr, plagioclase (which along with clinopyroxene typically makes up most of the residue for leached tholeiites; e.g. Mahoney, 1987), was largely replaced by secondary feldspar in these rocks

Table 1: Nd and Sr isotopic ratios and isotope-dilution abundances

Sample		Age (Ma)	Nd (ppm)	Sm	Sr	Rb	$^{147}Sm/^{144}Nd$	$^{87}Rb/^{86}Sr$	$(^{143}Nd/^{144}Nd)_0$	$(^{87}Sr/^{86}Sr)_0$	$\varepsilon_{Nd}(t)$	$(^{87}Sr/^{86}Sr)_t$
Old Pacific MORB												
Alexander I.												
KG 2988-7E	U	200	14·94	4·034	282·0	43·1	0·1632	0·4414	0·512930	0·70421	+6·5	0·70295
KG 3513-4	U	150	10·20	3·138	151·9	5·07	0·1859	0·0965	0·512975	0·70431	+6·7	0·70410
KG 3513-27	L	150	2·463	1·003	184·4	16·0	0·2463	0·2504	0·513091	0·70472	+7·8	0·70419
	U		7·674	2·611	156·5	10·8	0·2056	0·2000	0·513052	0·70482	+7·9	0·70439
KG 3981-2E	L	150			84·60	13·8		0·4722		0·70509		0·70408
	U		17·96	5·064	82·24	15·6	0·1704	0·5474	0·512893	0·70528	+5·4	0·70411
KG 3999-2	U	150	8·045	3·077	45·99	11·0	0·2312	0·6944	0·513117	0·70531	+8·6	0·70383
Old Western Indian Ocean												
Drill sites												
249-33-1(31)	U	140	8·502	2·522	108·8	4·27	0·1793	0·1134	0·512825	0·70412	+3·9	0·70389
249-33-3(115)	U	140	2·611	0·8938	99·43	0·508	0·2069	0·0148	0·512876	0·70368	+4·4	0·70365
250A-25-3(128)	U	90	6·970	2·496	126·8	8·20	0·2165	0·1871	0·513092	0·70316	+8·6	0·70292
250A-26-5(64)	U	90	9·796	2·608	236·4	1·12	0·1609	0·0137	0·512938	0·70301	+6·2	0·70299
690C-24-1(109)	U	85	77·56	12·93	1724	47·2	0·1008	0·0792	0·512557	0·70386	−0·6	0·70376
239-20-1(127)	L	72	2·966	1·489	111·3	4·25	0·3035	0·1105	0·513190	0·70295	+9·7	0·70284
	U		8·624	3·224	118·8	6·46	0·2259	0·1574	0·513129	0·70348	+9·3	0·70332
248-17-2(63)	L	72	4·026	1·377	187·0	1·02	0·2067	0·0157	0·512799	0·70432	+3·0	0·70431
	U		17·76	4·999	196·6	3·08	0·1702	0·0545	0·512768	0·70438	+2·7	0·70432
235-20-5(73)	U	70	4·604	1·747	99·97	1·00	0·2293	0·0290	0·513074	0·70305	+8·2	0·70302
245-19-1(01)	L	65	1·864	1·122	36·25	2·86	0·3639	0·2283	0·513153	0·70309	+8·6	0·70287
	U		6·208	2·534	68·96	7·99	0·2468	0·3349	0·513104	0·70362	+8·6	0·70331
236-33-3(116)	Glass	60	3·117	1·190	55·64	1·25	0·2308	0·0651	0·513030	0·70345	+7·4	0·70339
	U		2·879	1·106	55·16	1·14	0·2322	0·0599	0·513016	0·70352	+7·1	0·70347
236-34-2(123)	L	60	1·718	0·7133	62·81	1·33	0·2510	0·0613	0·513013	0·70350	+6·9	0·70345
	U				69·66	1·37		0·0567		0·70404		0·70399
240-7-1(60)	U	60	4·750	1·816	72·80	5·65	0·2310	0·2245	0·513153	0·70350	+9·8	0·70331
240-7-1(97)	L	60	2·130	1·040	66·20	4·59	0·2951	0·2003	0·513206	0·70294	+10·3	0·70277
	U		3·590	1·427	68·61	1·93	0·2402	0·0815	0·513197	0·70337	+10·5	0·70330
223-40-2(48)	L	60	3·189	1·408	81·03	18·1	0·2669	0·6453	0·513049	0·70391	+7·4	0·70336
	U		3·334	1·238	110·1	22·2	0·2241	0·5828	0·513039	0·70446	+7·6	0·70396
224-11-cc	U	55	33·32	6·777	621·4	12·8	0·1229	0·0597	0·512783	0·70362	+3·3	0·70357
221-19-2(81)	Glass	46	6·760	2·561	68·10	1·58	0·2290	0·0671	0·513055	0·70294	+7·9	0·70290

Table 1: continued

Sample		Age (Ma)	Nd (ppm)	Sm	Sr	Rb	$^{147}Sm/^{144}Nd$	$^{87}Rb/^{86}Sr$	$(^{143}Nd/^{144}Nd)_0$	$(^{87}Sr/^{86}Sr)_0$	$\varepsilon_{Nd}(t)$	$(^{87}Sr/^{86}Sr)_t$
Tethyan basalts												
Masirah												
MSX-75	L	150	3·731	1·576	32·39	0·115	0·2552	0·0103	0·513161	0·70305	+9·0	0·70302
	U		4·310	1·699	46·47	0·118	0·2382	0·0074	0·513158	0·70455	+9·3	0·70453
MSX-134	L	150	7·168	2·308	159·1	2·18	0·1946	0·0397	0·513071	0·70318	+8·4	0·70310
	U		10·25	3·089	202·4	2·47	0·1821	0·0353	0·513054	0·70352	+8·4	0·70345
MSX-158	L	150			108·9	0·193		0·0051		0·70291		0·70289
	U		6·787	2·171	145·5	0·273	0·1933	0·0054	0·512966	0·70334	+6·4	0·70333
MSX-171	L	150			39·67	0·111		0·0081		0·70307		0·70305
	U		4·567	1·783	60·71	0·128	0·2362	0·0061	0·513132	0·70467	+8·8	0·70466
MSX-239	L	150			121·0	2·00		0·0479		0·70318		0·70308
	U		7·040	2·453	167·8	2·16	0·2106	0·0372	0·513043	0·70420	+7·6	0·70412
MA-401	L	150	5·554	2·042	158·6	20·7	0·2222	0·3768	0·513033	0·70431	+7·2	0·70351
	U		6·302	2·238	156·5	24·6	0·2146	0·4543	0·513035	0·70451	+7·4	0·70354
MSX-71g	Plag	150	0·2057	0·0574	264·5	0·308	0·1687	0·0034	0·513076	0·70336	+9·0	0·70335
P-20	U	150	10·69	3·267			0·1847		0·513023		+7·7	
P-24	U	150	9·170	2·960			0·1947		0·513041		+7·9	
F-23g	U	150	0·3280	0·0734			0·1353		0·513022		+8·6	
F-24g	U	150	0·2584	0·0639			0·1494		0·513133		+10·5	
MSX-29E	L	120	25·39	5·605	330·0	20·3	0·1335	0·1777	0·512897	0·70314	+6·0	0·70284
	U		25·36	5·451	318·9	26·6	0·1300	0·2411	0·512921	0·70345	+6·5	0·70304
MSX-219E	L	120	15·45	4·364	67·69	0·690	0·1708	0·0295	0·512881	0·70435	+5·1	0·70430
	U		49·34	9·797	88·32	0·977	0·1200	0·0320	0·512850	0·70450	+5·3	0·70445
MSX-222E	L	120			698·8	105		0·4342		0·70455		0·70381
	U		23·59	4·786	565·5	41·4	0·1226	0·2116	0·512827	0·70459	+4·8	0·70423
F-54E	U	120	20·38	2·786			0·0826		0·512700		+2·9	
F-70E	U	120	24·96	5·240			0·1269		0·512845		+5·1	
I-669E	U	120	40·24	6·610			0·0993		0·512819		+5·0	
J-53E	U	120	70·56	13·97			0·1196		0·512732		+3·0	
J-179E	U	120	28·66	5·770			0·1217		0·512873		+5·7	
Z-114E	U	120	26·02	5·261			0·1222		0·512814		+4·5	
Z131E	U	120	47·88	8·502			0·1073		0·512774		+4·0	

Sample		Age (Ma)	Nd (ppm)	Sm	Sr	Rb	$^{147}Sm/^{144}Nd$	$^{87}Rb/^{86}Sr$	$(^{143}Nd/^{144}Nd)_0$	$(^{87}Sr/^{86}Sr)_0$	$\varepsilon_{Nd}(t)$	$(^{87}Sr/^{86}Sr)_t$
Yarlung–Zangpo (Xigaze)												
YZS-1	L	110			182·2	13·2		0·2088		0·70412		0·70380
	U		4·005	1·515	118·9	5·53	0·2287	0·1344	0·513095	0·70418	+8·4	0·70397
YZS-2	L	110			133·1	3·89		0·0845		0·70419		0·70406
	U		6·246	2·274	105·8	4·14	0·2200	0·1132	0·513075	0·70428	+8·2	0·70410
YZS-3	L	110			153·4	13·7		0·2579		0·70432		0·70391
	U		4·224	1·603	130·9	11·2	0·2294	0·2485	0·513098	0·70446	+8·5	0·70407
YZS-6	L	110			140·0	4·11		0·0850		0·70408		0·70395
	U		9·214	3·173	130·3	4·07	0·2082	0·0905	0·513059	0·70410	+8·0	0·70395
YZS-7	L	110			130·9	6·61		0·1461		0·70406		0·70383
	U		7·922	2·793	109·5	6·56	0·2131	0·1734	0·513066	0·70421	+8·1	0·70394
YZS-11	L	110			129·1	0·622		0·0139		0·70407		0·70405
	U		8·160	2·846	116·3	7·66	0·2148	0·1904	0·513075	0·70425	+8·2	0·70395

U, unleached split, but chips hand-picked and acid-cleaned; L, strongly acid-leached powder; Plag, plagioclase separate; g, gabbro. E suffix indicates E-MORB or ocean-island-type composition. Isotopic fractionation corrections are $^{148}NdO/^{144}NdO = 0{\cdot}242436$ ($^{148}Nd/^{144}Nd = 0{\cdot}241572$), $^{86}Sr/^{88}Sr = 0{\cdot}1194$. Data are reported relative to a value of $^{143}Nd/^{144}Nd = 0{\cdot}511850$ for the La Jolla Nd standard, and $^{87}Sr/^{86}Sr = 0{\cdot}71024$ for NBS 987 Sr. The total range measured for NBS 987 Sr is $\pm 0{\cdot}00002$ (last 2 years); for La Jolla Nd it is $\pm 0{\cdot}000011$ (0·2 ε units) in Hawaii and $\pm 0{\cdot}000025$ in Bern. Within-run errors on the isotopic data above are less than or equal to the external uncertainties on these standards. Total blanks: <60 pg for Sr, <15 pg for Nd in Hawaii and <170 pg in Bern. Uncertainties on Nd and Sm abundances are estimated at <0·2%, on Sr, <0·5%, and on Rb, ~1% for Hawaii data; for Bern data, $^{147}Sm/^{144}Nd$ uncertainty is <0·3%. Data for F-24 are from Nägler & Frei (1997); data for the Site 221 glass are from Mahoney *et al.* (1989). $\varepsilon_{Nd}(t) = 0$ today corresponds to $^{143}Nd/^{144}Nd = 0{\cdot}512640$; $\varepsilon_{Nd}(t) = 0$ for past times is calculated assuming $^{147}Sm/^{144}Nd = 0{\cdot}1967$. Ages of Alexander Island, Masirah, and Yarlung–Zangpo samples are from references cited in text; ages of drill-site samples are from the relevant Deep Sea Drilling Project or Ocean Drilling Program volume for each site. Site numbers are indicated at beginning of sample number [e.g. 249-33-3(115) is Site 249, core 33, section 3, 115 cm].

Table 2: Pb isotopic ratios and isotope-dilution abundances

Sample		Age (Ma)	Pb (ppm)	U	Th	$^{238}U/^{204}Pb$	$^{232}Th/^{204}Pb$	Th/U	$(^{206}Pb/^{204}Pb)_0$	$(^{207}Pb/^{204}Pb)_0$	$(^{208}Pb/^{204}Pb)_0$	$(^{206}Pb/^{204}Pb)_t$	$(^{207}Pb/^{204}Pb)_t$	$(^{208}Pb/^{204}Pb)_t$
Old Pacific MORB														
Alexander I.														
KG 2988-7E	U	200	0·7713	0·218	0·692	18·5	60·6	3·17	19·771	15·625	39·324	19·187	15·596	38·721
KG 3513-4	U	150	0·5738	0·0814	0·136	9·16	15·9	1·68	19·354	15·616	38·788	19·138	15·605	38·670
KG 3513-27	L	150	0·1112	0·0358	0·0866	18·7	46·7	2·42	19·418	15·574	38·794	18·978	15·552	38·446
	U		0·3097	0·0980	0·294	20·5	63·4	3·00	19·389	15·593	38·866	18·907	15·569	38·393
KG 3981-2E	U	150	0·8495	0·397	1·28	30·6	102	3·23	19·735	15·582	39·487	19·015	15·547	38·726
KG 3999-2	U	150	0·1211	0·0703	0·169	37·9	93·9	2·40	19·819	15·589	39·097	18·928	15·545	38·398
Old Western Indian Ocean														
Drill sites														
249-33-1(31)	U	140	1·390	0·330	1·42	15·4	66·7	4·29	18·188	15·553	38·606	17·858	15·537	38·142
249-33(115)	U	140	1·005	0·310	1·00	19·5	65·3	3·24	18·128	15·554	38·553	17·700	15·533	38·099
250A-25-3(128)	U	90	0·1975	0·0868	0·1202	27·9	39·9	1·38	18·696	15·514	38·169	18·304	15·495	37·991
250A-26-5(64)	U	90	0·7651	0·113	0·756	9·59	66·3	6·69	19·322	15·585	39·195	19·187	15·579	38·899
690C-24-1(109)	U	85	9·099	1·04	1·90	7·03	13·3	1·83	17·491	15·496	37·501	17·398	15·492	37·445
239-20-1(127)	L	72	0·1175	0·0075	0·0060	3·94	3·23	0·79	17·593	15·428	37·348	17·549	15·426	37·336
	U		0·3776	0·0580	0·0921	9·51	15·6	1·59	17·759	15·452	37·468	17·652	15·447	37·412
248-17-2(63)	L	72	0·4975	0·136	0·370	17·6	49·4	2·72	18·596	15·658	39·141	18·400	15·649	38·965
	U		1·997	0·251	0·993	8·06	33·0	3·96	18·577	15·630	38·957	18·487	15·626	38·839
235-20-5(73)	U	70	0·2533	0·0326	0·0890	8·07	22·7	2·73	18·131	15·456	37·876	18·043	15·452	37·797
245-19-1(01)	L	65	0·0560	0·0154	0·0106	17·2	12·2	0·69	18·353	15·467	37·587	18·178	15·459	37·548
	U		0·2408	0·0547	0·129	14·4	35·0	2·36	18·586	15·577	38·107	18·440	15·570	37·994
236-33-3(116)	Glass	60	0·3704	0·0496	0·154	8·67	27·8	3·11	19·364	15·627	38·893	19·283	15·623	38·810
	U		0·5434	0·0454	0·140	5·39	17·2	3·08	19·191	15·630	38·854	19·141	15·628	38·803
236-34-2(123)	L	60	0·1480	0·0103	0·0232	4·47	10·3	2·24	18·662	15·591	38·770	18·620	15·589	38·739
	U		0·6857	0·0290	0·114	2·70	10·9	3·92	18·601	15·573	38·689	18·576	15·572	38·656
240-7-1(60)	U	60	0·2210	0·0536	0·117	15·3	34·5	2·18	18·457	15·514	38·191	18·314	15·507	38·080
240-7-1(97)	L	60	0·0440	0·0369	0·0117	53·5	17·6	0·32	19·045	15·543	38·219	18·545	15·519	38·167
	U		0·2294	0·126	0·0468	34·8	13·4	0·37	18·732	15·520	38·214	18·406	15·505	38·174
223-40-2(48)	L	60	0·1862	0·0863	0·0716	29·6	25·4	0·83	18·726	15·551	38·659	18·449	15·538	38·584
	U		0·9523	0·146	0·182	9·74	12·6	1·25	18·625	15·532	38·500	18·534	15·528	38·463
224-11-cc	U	55	1·977	0·782	3·00	25·3	100	3·84	18·675	15·504	38·819	18·458	15·494	38·546
221-19-2(81)	Glass	46	0·3387	0·0493	0·185	9·14	35·6	3·76	18·126	15·511	38·071	18·061	15·508	37·990

Sample		Age (Ma)	Pb (ppm)	U	Th	$^{238}U/^{204}Pb$	$^{232}Th/^{204}Pb$	Th/U	$(^{206}Pb/^{204}Pb)_0$	$(^{207}Pb/^{204}Pb)_0$	$(^{208}Pb/^{204}Pb)_0$	$(^{206}Pb/^{204}Pb)_t$	$(^{207}Pb/^{204}Pb)_t$	$(^{208}Pb/^{204}Pb)_t$
Tethyan basalts														
Masirah														
MSX-75	U	150	0·0686	0·0120	0·0372	11·1	35·7	3·11	18·807	15·544	38·443	18·545	15·531	38·177
MSX-134	L	150	0·0969	0·0941	0·439	64·5	311	4·66	19·870	15·579	40·400	18·352	15·505	38·084
	U		0·1802	0·121	0·557	44·2	209	4·59	19·519	15·615	39·752	18·479	15·564	38·192
MSX-158	U	150	0·0612	0·0753	0·370	83·7	425	4·92	20·608	15·645	41·382	18·638	15·548	38·214
MSX-171	U	150	0·0684	0·0131	0·0388	12·2	37·3	2·95	18·773	15·519	38·400	18·485	15·505	38·122
MSX-239	U	150	0·0729	0·0429	0·197	38·3	182	4·60	19·268	15·591	39·420	18·367	15·547	38·066
MA-401	L	150	0·1560	0·0752	0·153	30·8	64·6	1·91	18·911	15·524	38·501	18·187	15·488	38·019
	U		0·2503	0·0688	0·207	17·5	54·2	3·00	18·649	15·539	38·356	18·238	15·519	37·952
MSX-71g	Plag	150	0·1118	0·0200	0·0011	11·5	0·66	0·06	19·148	15·589	38·565	18·878	15·577	38·560
P-20	U	150	0·361	0·126	0·627	22·2	114	5·38	18·694	15·493	38·513	18·171	15·467	37·661
P-24	U	150	0·798	0·119	0·499	9·48	41·1	4·19	18·543	15·531	38·474	18·320	15·520	38·168
F-23g	U	150	0·164	0·0078	0·0075	3·08	3·00	0·943	18·392	15·515	38·134	18·320	15·511	38·112
F-24g	U	150	0·195	0·019	0·0396	6·17	13·3	2·08	18·488	15·511	38·299	18·343	15·504	38·200
MSX-29E	L	120	1·508	0·872	4·32	38·0	195	4·96	19·709	15·592	39·842	18·995	15·557	38·683
	U		1·717	1·01	4·49	38·6	177	4·44	19·575	15·581	39·689	18·850	15·546	38·634
MSX-219E	U	120	2·320	2·32	11·8	67·2	354	5·09	20·158	15·629	40·903	18·895	15·568	38·797
MSX-222E	U	120	2·299	1·13	3·39	32·1	99·4	3·00	19·508	15·581	39·403	18·905	15·552	38·811
F-54E	U	120	3·041	3·41	18·7	73·0	413	5·48	19·189	15·514	39·662	17·818	15·448	37·200
F-70E	U	120	1·121	0·813	2·71	47·2	162	3·33	19·838	15·602	39·268	18·951	15·559	38·303
I-669E	U	120	2·168	1·33	6·69	40·0	208	5·04	19·562	15·599	39·742	18·810	15·563	38·503
J-53E	U	120	2·461	1·19	7·15	31·6	196	6·00	19·427	15·561	39·506	18·833	15·532	38·340
J-179E	U	120	0·829	0·834	4·45	65·3	367	5·45	18·939	15·518	39·639	17·712	15·459	37·451
Z-114E	U	120	1·238	0·929	3·38	48·5	182	3·64	19·403	15·561	39·253	18·492	15·517	38·169
Z131E	U	120	1·457	3·10	13·3	142	632	4·30	20·404	15·610	40·409	17·728	15·480	36·645

Table 2: continued

Sample location		Age (Ma)	Pb (ppm)	U	Th	$^{238}U/^{204}Pb$	$^{232}Th/^{204}Pb$	Th/U	$(^{206}Pb/^{204}Pb)_0$	$(^{207}Pb/^{204}Pb)_0$	$(^{208}Pb/^{204}Pb)_0$	$(^{206}Pb/^{204}Pb)_t$	$(^{207}Pb/^{204}Pb)_t$	$(^{208}Pb/^{204}Pb)_t$
Yarlung–Zangpo (Xigaze)														
YZS-1	U	110	0·3837	0·0853	0·0375	13·8	6·25	0·44	17·771	15·427	37·417	17·534	15·416	37·383
YZS-2	U	110	0·6177	0·108	0·0763	10·7	7·88	0·71	17·704	15·411	37·351	17·519	15·402	37·308
YZS-3	U	110	0·4667	0·0654	0·0506	8·67	6·93	0·77	17·697	15·426	37·421	17·548	15·419	37·383
YZS-6	U	110	0·2712	0·0644	0·102	14·7	23·9	1·58	17·726	15·413	37·432	17·473	15·401	37·301
YZS 7	U	110	0·2450	0·0807	0·0827	20·4	21·6	1·02	17·765	15·409	37·388	17·415	15·392	37·270
YZS-11	U	110	0·2994	0·0546	0·0894	11·2	19·0	1·64	17·630	15·404	37·369	17·436	15·395	37·265

Pb isotope ratios are corrected for fractionation using the NBS 981 standard values of Todt *et al.* (1996); the total ranges measured for NBS 981 are ±0·011 for $^{206}Pb/^{204}Pb$, ±0·010 for $^{207}Pb/^{204}Pb$, and ±0·032 for $^{208}Pb/^{204}Pb$ (last 2 years). Within-run uncertainties (2 SE) on the isotopic data above are less than these values. Estimated uncertainty on Pb abundances ~0·5%, on U ~1%, and on Th <2%. Propagation of errors on age-corrected Pb isotope ratios: for a 150 Ma sample with $^{238}U/^{204}Pb = 30$ and $^{232}Th/^{204}Pb = 100$, a maximum error on parent–daughter ratios translates to an additional error of ±0·011 on $(^{206}Pb/^{204}Pb)_t$, ±0·005 on $(^{207}Pb/^{204}Pb)_t$, and ±0·019 on $(^{208}Pb/^{204}Pb)_t$. Total procedural blanks: Pb 4–34 pg in Hawaii and <70 pg in Bern; U <5 pg in Hawaii and <30 pg in Bern; Th <3 pg.

during alteration (Doubleday *et al.*, 1994) and that little material with pristine $^{87}Sr/^{86}Sr$ remains.

Unlike Sr isotopes, the age-corrected Nd and Pb isotopic data all fall in a restricted field within the Pacific–North Atlantic MORB mantle array in Fig. 4c and d, particularly when the modern array is adjusted to the approximate position it would have occupied at 150 Ma (assuming the only changes have been caused by radioactive decay of parent nuclides in the MORB source mantle). The data plot in the low-ε_{Nd}, high-$^{206}Pb/^{204}Pb$, high-$^{208}Pb/^{204}Pb$ region of this array. Values of $(^{207}Pb/^{204}Pb)_t$ lie within the range for MORB and oceanic islands as well (Fig. 5a). The one sample for which we determined Nd and Pb isotopes on both acid-leached and unleached splits (KG 3513-27) has identical $\varepsilon_{Nd}(t)$, within errors, for each split, at +7·8 and +7·9; leaching also produced only small changes in the age-adjusted Pb isotope ratios of this sample [e.g. $(^{206}Pb/^{204}Pb)_t$ of 18·98 and 18·91; see linked light and dark squares in Fig. 4]. Because the age-corrected Pb isotopic values of all the samples (1) plot in a small field within the narrow Pacific–North Atlantic MORB array in both panels c and d of Fig. 4 and (2) have a lesser total spread in $^{208}Pb/^{204}Pb$ and $^{206}Pb/^{204}Pb$ relative to the measured, present-day range (0·33 vs 0·70 and 0·28 vs 0·47, respectively; the range in $^{207}Pb/^{204}Pb$ is the same within analytical error), and because (3) values for the leached and unleached splits of KG 3513-27 agree well with each other, it appears that alteration affecting U/Pb or Th/Pb ratios mainly occurred within a few million years after eruption. The same appears to be true of most samples from the other localities studied (see below).

Western Indian Ocean drill sites

The drillhole samples display a wide range in elemental composition. Primitive-mantle-normalized incompatible element patterns of several samples are illustrated in Fig. 6, and can be seen to vary from typical N-MORB type (sloping generally downward to the left; e.g. Site 235-20-5) to E-MORB type (moderate upward slope to the left; e.g. Site 250A-26-5). The basalt from Site 690C (on Maud Rise) has an ocean-island-like pattern resembling those of Gough Island lavas (South Atlantic), including a spike at Ba and trough at Th and U; this rock is an unusual xenocryst-bearing alkalic basalt that Schandl *et al.* (1990) concluded originated from a hydrous source containing small amounts of phlogopite and apatite. The Site 224 sample shows somewhat similar, but less extreme, ocean-island-like features. In contrast, the pattern for a Site 249 lava has a sizeable trough at Nb and Ta (as well as a larger than usual peak at Pb), a characteristic commonly seen in lavas influenced by continental lithosphere, and in arc-related basalts, but

Table 3: Bulk-rock incompatible element abundances (ppm)

Sample	Rb	Ba	Th	U	Nb	Ta	La	Ce	Pr	Sr	Pb	Nd	Zr	Sm	Eu	Gd	Dy	Y	Ho	Er	Tm	Yb	Lu
Old Western Indian Ocean																							
249-33-3(115)	7·8	80	1·35	0·24	3·5	0·19	7·36	15·3	2·11	136	1·12	9·80	85	2·90	0·99	4·13	4·44	28·0	0·92	2·70	0·37	2·83	0·37
250A-26-5(64)	13	193	1·71	0·47	24	1·35	14·4	31·7	3·62	—	1·16	15·7	123	4·19	1·43	4·94	4·53	25·5	0·86	2·76	0·33	2·68	0·32
239-20-1(127)	6·3	9·7	0·10	0·04	1·1	0·08	2·33	7·60	1·40	—	0·39	8·03	87	3·13	1·16	4·81	5·56	33·8	1·07	3·64	0·46	3·71	0·50
248-17-2(65)	3·0	68	0·86	0·20	8·6	0·45	8·47	23·3	3·15	207	1·25	16·6	123	4·66	1·63	5·09	5·36	28·7	1·02	2·83	0·37	2·55	0·35
235-20-5(73)	2·0	4·5	0·04	0·03	1·1	0·06	2·04	6·39	1·12	135	0·30	6·38	68	2·27	0·95	3·25	4·20	25·5	0·82	2·53	0·34	2·60	0·35
245-19-1(01)	6·8	5·1	0·04	0·09	0·87	—	1·46	5·18	1·00	86	0·23	6·43	57	2·57	0·97	3·79	5·11	32·0	1·07	3·28	0·47	3·23	0·44
236-33-3(117)	5·5	7·8	0·14	0·05	1·9	0·13	1·84	4·69	0·70	103	0·20	3·96	39	1·26	0·60	2·07	2·81	16·1	0·58	1·85	0·25	1·75	0·24
240-7-1(97)	18	16	0·06	0·04	1·5	0·09	1·96	5·41	0·91	89	0·37	5·48	54	1·88	0·85	2·91	3·74	24·3	0·78	2·57	0·33	2·58	0·35
223-40-2(48)	17	82	0·27	0·11	4·4	0·25	4·96	12·6	1·75	269	0·71	9·52	78	2·58	1·05	3·63	4·26	24·9	0·86	2·44	0·36	2·29	0·33
224-11-cc	28	692	4·28	1·12	47	3·31	52·6	98·1	11·1	750	2·66	44·8	268	8·69	3·04	9·58	6·36	32·7	1·10	3·03	0·37	2·50	0·36
Masirah																							
MSX-75	0·15	4·1	0·07	0·03	0·91	0·06	1·21	4·00	0·78	65	0·18	4·64	47	1·95	0·65	2·80	4·06	21·3	0·76	2·49	0·35	2·55	0·37
MSX-134	2·3	50	0·58	0·18	8·4	0·55	6·56	14·9	2·10	200	0·36	10·6	78	3·41	1·15	3·88	4·82	24·4	0·91	2·75	0·37	2·41	0·32
MSX-158	0·35	23	0·38	0·11	5·2	0·34	4·21	9·61	1·42	175	0·21	6·97	50	2·23	0·85	2·73	3·42	18·1	0·69	1·92	0·26	1·89	0·25
MSX-239	2·0	46	0·17	0·06	3·3	0·22	3·22	8·53	1·41	—	0·22	7·08	60	2·55	0·98	3·50	3·94	23·5	0·86	2·53	0·36	2·28	0·33
MA-401	22	280	0·25	0·09	2·7	0·19	2·63	6·99	1·15	200	0·43	6·64	57	2·31	0·84	3·14	3·80	21·2	0·77	2·32	0·36	2·15	0·32
MSX-29E	30	404	4·30	0·89	48	2·87	31·3	57·4	6·55	299	2·07	27·2	180	6·04	1·91	6·25	5·89	32·4	1·12	3·17	0·43	3·01	0·40
MSX-219E	1·7	34	8·24	1·93	75	4·38	52·8	96·5	11·1	70	2·32	41·0	300	8·68	1·59	8·34	8·43	45·8	1·62	5·14	0·74	5·10	0·70
Standard																							
BHVO-1 meas.	9·5	136	1·09	0·41	18·6	1·11	15·7	40·3	5·21	416	2·13	24·7	181	6·17	2·14	6·51	5·24	25·8	0·85	2·48	0·30	2·05	0·28
BHVO-1 rec.	9·7	133	1·233	0·41	19·0	1·16	15·8	37·8	5·40	420	2·051	24·8	179	6·10	1·98	6·40	5·20	27·1	0·99	2·40	0·33	2·02	0·29

At the 0·2–1 ppm abundance level in the rock, the relative precision for most elements is 3·5% or better (range is 1·2% to 5·0%). An indication of accuracy is given by measured (meas.) and recommended (rec.) values for the BHVO-1 standard. The recommended values for BHVO-1 are principally from Govindaraju (1989); those for Th and Pb are isotope-dilution measurements by thermal ionization mass spectrometry made at the University of Hawaii.

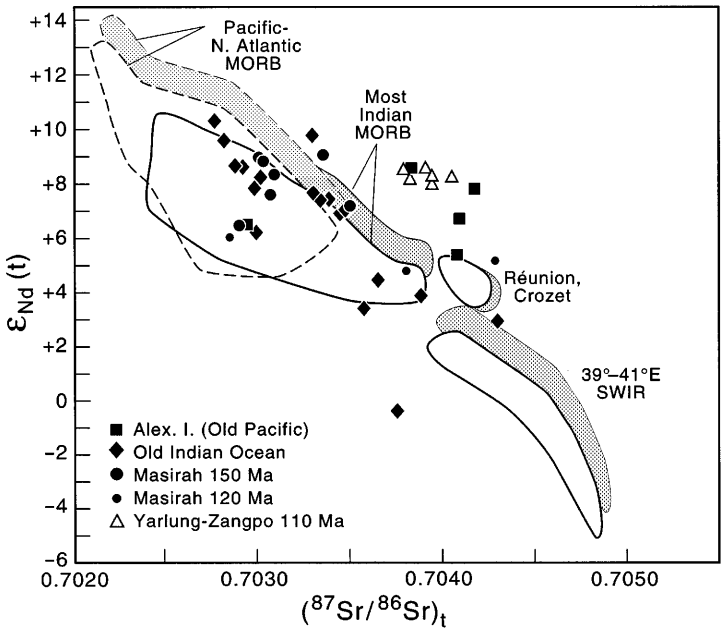

Fig. 3. Age-corrected $\varepsilon_{Nd}(t)$ vs $(^{87}Sr/^{86}Sr)_t$. It should be noted that not all samples were acid-leached and that for samples with data on both unleached and acid-leached or glass splits, only values for leached or glass splits are shown. Present-day fields for Pacific–North Atlantic MORB, Indian MORB [including the 39°–41°E section of the Southwest Indian Ridge (SWIR)], and Réunion and Crozet hotspot volcanoes are shaded; the adjacent unshaded fields are positioned for 150 Ma, assuming the modern MORB and Réunion–Crozet mantle sources have average $^{147}Sm/^{144}Nd$ of 0·24 and 0·17, and $^{87}Rb/^{86}Sr$ 0·02 and 0·10, respectively (see Peng & Mahoney, 1995). Data sources for the fields are as in Fig. 1 and, for Réunion and Crozet, W. M. White (unpublished data, 1993) and Mahoney *et al.* (1996, and references therein).

rarely in either fresh or altered oceanic basalts (compare Site 248 pattern). Patterns of the visibly fresher N- and E-MORB samples (e.g. Site 236-33-3, Site 250A-26-5) are relatively smooth, and even the more altered samples lack the pronounced spikes or troughs seen for some elements in patterns of highly altered basalts (Bienvenu *et al.*, 1990; Staudigel *et al.*, 1995; Jochum & Verma, 1996). Alteration effects are most evident in a marked elevation of Rb in the N-MORB lavas; Ba is also elevated significantly in many of these lavas (e.g. the Site 223 sample). Small peaks or troughs, which may reflect alteration, are present at Pb in several patterns, whereas U peaks and/or low Th/U ratios indicate significant U uptake in several samples (e.g. Site 245-19-1).

We determined Sr and Pb isotopes on both unleached and leached (or glass) splits of seven of the drill-core basalts studied and Nd isotopes on six pairs. The $(^{87}Sr/^{86}Sr)_t$ values of all but one of the leached splits are significantly lower (by as much as 0·0006) than those of the unleached splits, whereas only negligible differences are observed in $\varepsilon_{Nd}(t)$ (0–0·4 epsilon units). The differences in age-corrected Pb isotope ratios for the members of each unleached–leached (or glass) pair are also relatively small, with one exception (see linked symbols in Fig. 4a and b). For example, the difference in $(^{206}Pb/^{204}Pb)_t$ ranges from 0·04 to 0·14, except for sample 245-19-1, which shows a difference of 0·26, by far the largest observed for any of the samples in our study. As with Nd isotopes, the age-corrected Pb isotope ratios of an unleached split can be either slightly higher or lower than for the corresponding leached residue or glass separate. Values of $(^{207}Pb/^{204}Pb)_t$ are all within the range for MORB and ocean islands (Fig. 5a), except for sample 248-17-2, for which both leached and unleached splits have high $(^{207}Pb/^{204}Pb)_t$ (15·65, 15·63) relative to $(^{206}Pb/^{204}Pb)_t$ (18·40, 18·49). Abundances of Nd, Sm, Pb, U, Th, and Rb typically dropped substantially with leaching. Although the $^{147}Sm/^{144}Nd$ ratios of leached splits tend to be higher than for their unleached counterparts, consistent with a relative enrichment of clinopyroxene in most of these residues (e.g. Mahoney, 1987), the $^{238}U/^{204}Pb$ and $^{232}Th/^{204}Pb$ values can be either higher or lower, probably depending on the particular combination of altered and unaltered phases remaining in the leached residue. It is important to note that, except in the glasses, neither set of values necessarily corresponds to those in the pristine rock.

The total range in $\varepsilon_{Nd}(t)$ (unless otherwise specified, in the text hereafter we use isotopic values for leached residues or glass, when available) is considerable: +10·3 to –0·6. That for $(^{87}Sr/^{86}Sr)_t$ is also large, from 0·70277 to 0·70431. In contrast to the Alexander Island basalts, most of the age-adjusted drillhole-basalt data plot within or very close to the MORB fields in the Nd–Sr isotope

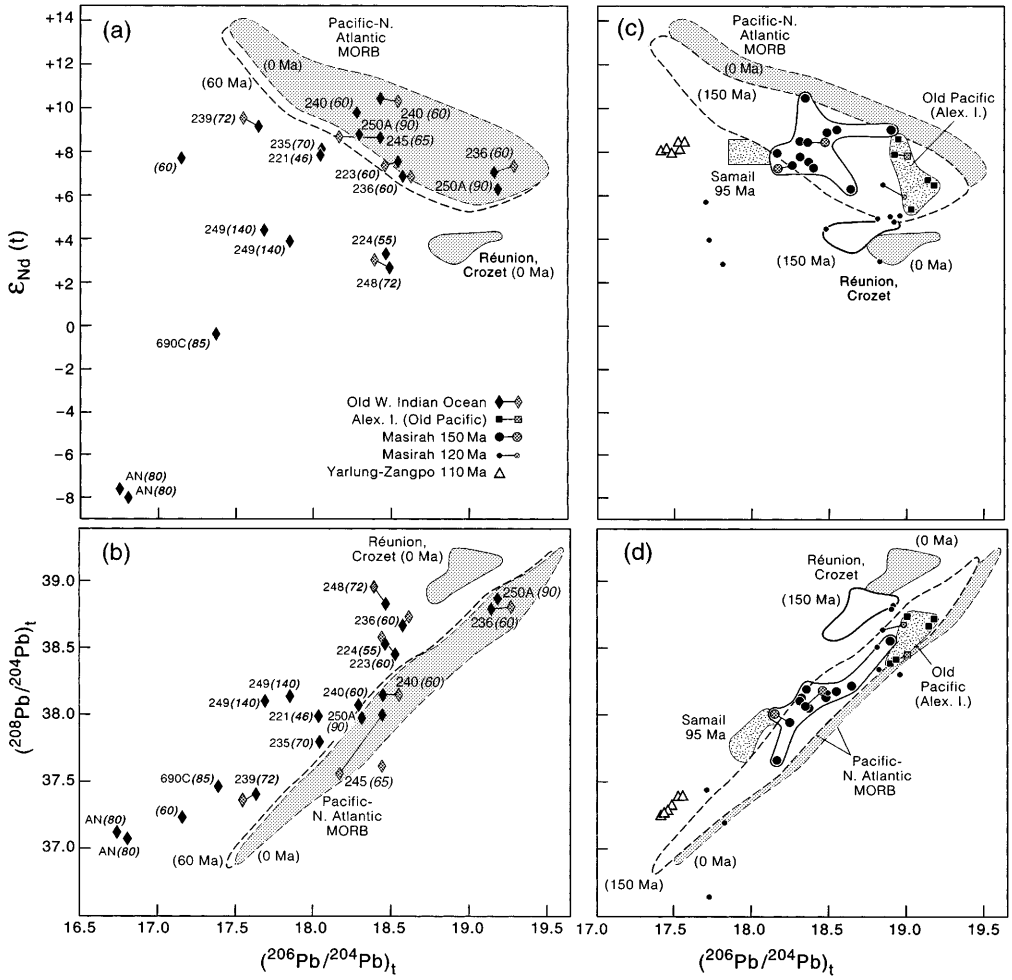

Fig. 4. Age-corrected $\varepsilon_{Nd}(t)$ (a, c) and $(^{208}Pb/^{204}Pb)_t$ (b, d) vs $(^{206}Pb/^{204}Pb)_t$. Acid-leached (or glass) and unleached pairs are indicated by light and dark symbols, respectively, linked by tie lines. As in Fig. 3, the field for the modern Pacific–North Atlantic MORB source at 150 Ma (c, d) and 60 Ma (a, b) is unshaded, and additionally assumes an average $^{238}U/^{204}Pb = 5$ and $^{232}Th/^{238}U = 2{\cdot}3$ in the source mantle (White, 1993); that for the Réunion–Crozet field at 150 Ma (c, d) is also unshaded and assumes source values of 12 and 3·3, respectively (Peng & Mahoney, 1995). Site numbers are shown adjacent to data points in (a) and (b), with ages in parentheses. Diamonds labeled AN at $\varepsilon_{Nd}(t)$ ~–8 are for Afanasy-Nikitin Seamount (Mahoney *et al.*, 1996); that at $(^{206}Pb/^{204}Pb)_t$ ~17·2 is for a seamount southwest of Afanasy-Nikitin estimated at 60 Ma (our unpublished data, 1997). Field for Samail ophiolite is from data of Chen & Pallister (1981) (for Pb isotopes) and McCulloch *et al.* (1981) [for $\varepsilon_{Nd}(t)$].

diagram (Fig. 3). An interesting exception is the chemically and petrographically unusual alkalic lava from Site 690C (Schandl *et al.*, 1990) on Maud Rise, which may have formed in association with a jump of the ancestral Southwest Indian Ridge toward the Bouvet hotspot in the 85–100 Ma period (e.g. Barker *et al.*, 1990); this sample has anomalously low $(^{87}Sr/^{86}Sr)_t$ (0·70376) for its low $\varepsilon_{Nd}(t)$ (–0·6).

Pb isotopes also exhibit a wide range, with $(^{206}Pb/^{204}Pb)_t$, varying from 17·40 (the Site 690C sample) to 19·28 (the Site 236 glass). Many of the old western Indian Ocean basalts resemble modern Indian MORB and hotspot islands in that their age-corrected Pb and Nd isotopic ratios place them on the low-$^{206}Pb/^{204}Pb$ side of the Pacific–North Atlantic MORB-source field in Fig. 4a and b. The oldest lavas, from Site 249, were erupted at ~140 Ma during early spreading between Africa and southern Greater Indo-Madagascar, and display a strong Indian-Ocean-type signature in both Fig. 4a and b. Samples from Sites 690C, 239, 248, 235, 224, and 221, with ages between ~85 and 46 Ma, also have clear Indian-Ocean-type isotopic signatures. In addition, dredged lavas from Afanasy-Nikitin Seamount (Fig. 2), erupted on or near the western Southeast Indian Ridge at ~80 Ma in a location far from continental landmasses, recently have been shown to possess lower $\varepsilon_{Nd}(t)$ (–8) and $(^{206}Pb/^{204}Pb)_t$

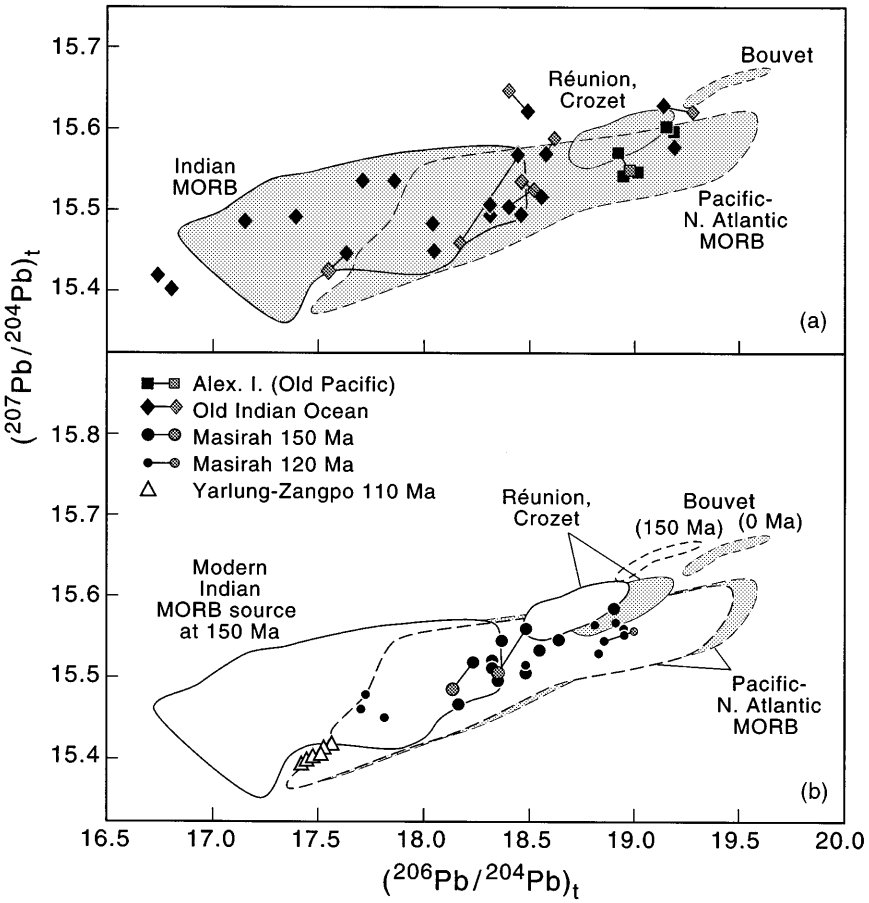

Fig. 5. Age-corrected $(^{207}Pb/^{204}Pb)_t$ vs $(^{206}Pb/^{204}Pb)_t$. Symbols, fields, and data sources are as in Figs 3 and 4, plus Sun (1980) for Bouvet.

(16·77) values than any modern Indian Ocean (or any other oceanic) lavas (see Fig. 4). Thus, Indian-MORB-type isotopic compositions clearly were present in the old western Indian Ocean mantle, in good agreement with results for old lavas from the eastern Indian Ocean (Lanyon, 1995; Pyle *et al.*, 1995; Weis & Frey, 1996).

However, data for several sites overlap the Pacific–North Atlantic MORB-source array. As noted earlier, such characteristics appear to be very rare within the main part of the Indian Ocean domain today (Fig. 1). The Site 250A samples (including an N-MORB and an E-MORB), the two flows we analyzed from Site 240, and the upper of two petrographically distinct units (Fisher *et al.*, 1974) at Site 236 have values that fall within the Pacific–North Atlantic MORB-source field in both Fig. 4a and b. The same is true for the Site 245 basalt, despite the significant difference in age-corrected Pb isotopic values between the leached and unleached splits of this sample. Moreover, the Site 250A-26-5 (90 Ma) E-MORB and the Site 236-33-3 glass–crystalline-rock pair (60 Ma) have age-corrected $(^{206}Pb/^{204}Pb)_t$ >19, significantly greater than seen for any modern Indian MORB (most of which have $^{206}Pb/^{204}Pb$ <18·4). [Although it was not age-corrected, an even higher present-day $^{206}Pb/^{204}Pb$ value of 19·580 was reported by Hart (1988) for a Site 250A lava deeper in the core than our E-MORB sample, with a value of 19·322.] Some modern Indian Ocean island lavas have values around 19, but they also have markedly lower ε_{Nd} (~ +4 or less vs +6·2 and +7·4), higher relative $^{208}Pb/^{204}Pb$, and usually higher $^{87}Sr/^{86}Sr$ (e.g. ~0·704 for Réunion and Crozet). Two samples display notably ambiguous 'mixed' isotopic characteristics, one from the lower unit at Site 236 and one from Site 223 (both ~60 Ma). In Fig. 4a, values for both the unleached and leached splits of these samples fall near the edge of but within the estimated Pacific–North Atlantic MORB-source array for 60 Ma. However, in Fig. 4b, data for both samples lie well above this field. Along the present-day spreading ridges, qualitatively similar mixed signatures have been found only in some lavas at the fringes of the Indian MORB domain (Mahoney *et al.*, 1992; Pyle *et al.*, 1992; Volker & *et al.*, 1993).

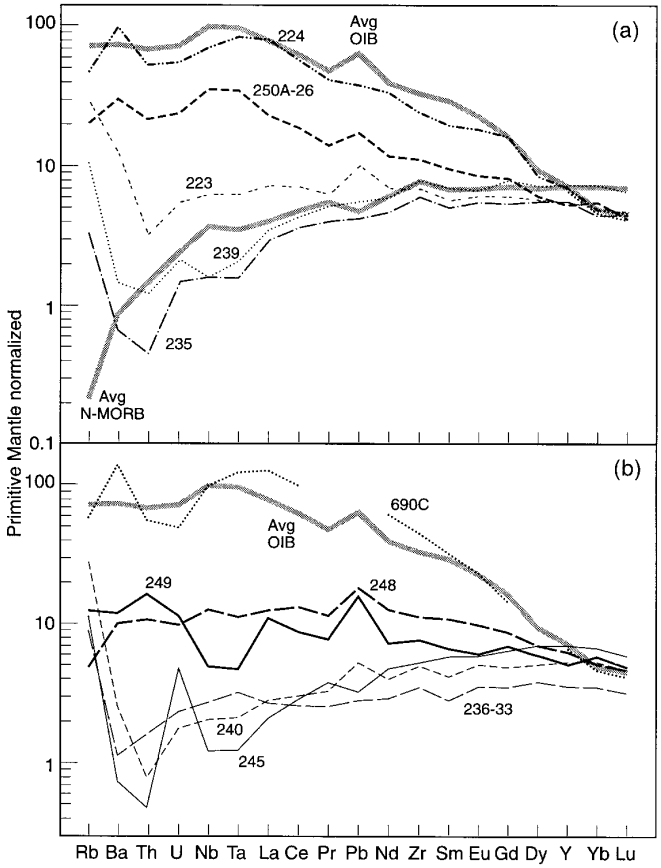

Fig. 6. Incompatible element patterns of several western Indian Ocean drillhole lavas. Shown for comparison are average N-MORB and oceanic island basalt (OIB) patterns. Arrangement into two panels is for clarity only. Primitive-mantle normalizing values and N-MORB and OIB averages are Sun & McDonough's (1989). The Site 690C pattern is from data of Schandl *et al.* (1990). The Ta value for the Site 245 pattern is inferred from the measured Nb value assuming Nb/Ta = 17.

Masirah

Masirah is an island off the coast of Oman that contains well-preserved exposures of uplifted abyssal oceanic crust. An older suite of MORB-type magmatic and ultramafic rocks is present, as well as a younger group of magmatic rocks, principally alkalic basalts and their differentiates but also amphibole–clinopyroxene gabbros and rare oceanic granites (e.g. Moseley & Abbotts, 1979; Abbotts, 1981; Moseley, 1990; Smewing *et al.*, 1991; Gnos & Perrin, 1996; Nägler & Frei, 1997). Recent dating reveals that the MORB-type suite is ~150 Ma, whereas the younger suite is ~120 Ma (Smewing *et al.*, 1991; Immenhauser, 1996; Nägler & Frei, 1997). The Masiran seafloor appears to have formed on the slow-spreading, transform-fault-dominated ridge system (e.g. Fisher *et al.*, 1986) linking the main Tethyan and early western Indian Ocean (northeastern Somali Basin) spreading centers in the narrow basin between northwestern Greater Indo-Madagascar and the northeastern corner of Arabia–Africa (see Fig. 7) (e.g. Mountain & Prell, 1990; Smewing *et al.*, 1991; G. Mountain, personal communication, 1993). (Note that the similar-age basement at Site 249 was formed in the Mozambique Basin farther southwest, to the southwest of Madagascar.) The cause of the later magmatism at ~120 Ma is uncertain but may be related to lithospheric fracturing and passage of the region near a hotspot (Meyer *et al.*, 1996; Nägler & Frei, 1997).

Primitive-mantle-normalized element patterns of representative tholeiitic and alkalic Masiran lavas (the latter represented by an E suffix in the tables) are shown in Fig. 8a and b. Low, MORB-like abundances of incompatible elements characterize the 150 Ma tholeiitic basalts, and their patterns range from typical N-MORB type to transitional-MORB type (relatively flat). The patterns of the 120 Ma alkalic lavas slope generally upward to the left and broadly resemble those of many oceanic island basalts [compare the average OIB pattern in Fig. 8; see also Meyer *et al.* (1996)]. Overall, the patterns are relatively smooth. However, Rb and Ba can be mildly to dramatically enriched or depleted relative

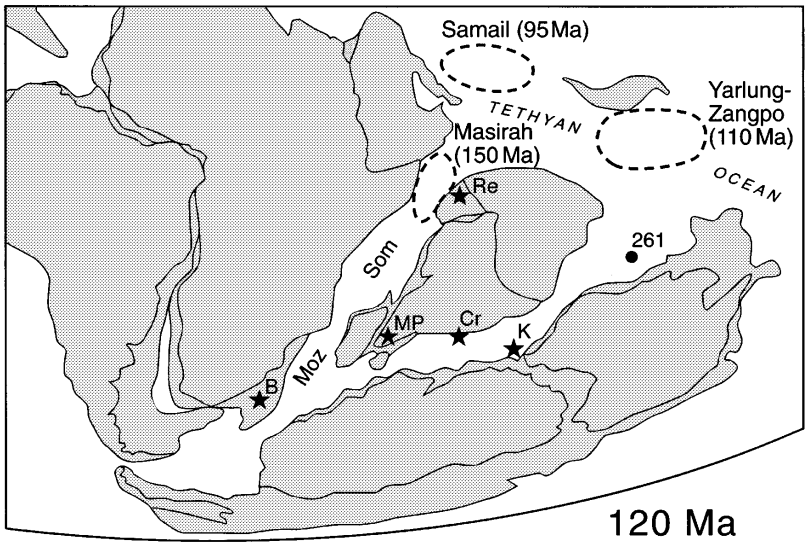

Fig. 7. Reconstruction at 120 Ma (after Lawver & Gahagan, 1993). Approximate 120 Ma location of Masiran crust is shown, along with that of Site 261 and positions of the present Réunion (Re), Bouvet (B), Crozet (Cr), Marion–Prince Edward (MP), and Kerguelen (K) hotspots. Rough indications of the location of the Yarlung–Zangpo and Samail crust are also shown. Moz, Mozambique Basin; Som, Somali Basin.

to Th in the visibly more altered samples analyzed (e.g. MA-401, MSX-219E). Small to moderate troughs or peaks at Pb are present in some patterns as well, and a substantial negative Eu anomaly can be seen in the pattern for MSX-219E, a trachytic lava.

As with the drillhole samples, acid-leaching of the Masiran rocks reduced their $(^{87}Sr/^{86}Sr)_t$ values while causing negligible changes in $\varepsilon_{Nd}(t)$ and only modest ones in age-corrected Pb isotope ratios. In several cases, a large reduction in $(^{87}Sr/^{86}Sr)_t$ occurred: for example, from 0·70466 to 0·70305 for MSX-171. In the Nd–Sr isotope diagram (Fig. 3), the data for most of the Masiran rocks plot in or very close to the estimated 150 Ma MORB-source field (in the broad area of this diagram where Pacific–North Atlantic and Indian fields overlap), although leaching failed to bring the Sr isotope values of MA-401 or MSX-219E into this field. The plagioclase separate—which we did not leach—of a gabbro (MSX-71g) also yielded higher $(^{87}Sr/^{86}Sr)_t$ (0·70335) than the leached splits of basalts MSX-75 and MSX-171 [with Sr isotopic values of ~0·7030 at similar $\varepsilon_{Nd}(t)$], evidently indicating that the plagioclase was somewhat affected by interaction with seawater.

For the 150 Ma samples, $\varepsilon_{Nd}(t)$ ranges from +10·5 to + 6·4, indicative of intrinsic heterogeneity in the mantle source; however, eight of the 11 samples have values between +9·0 and +7·6. Values of $(^{206}Pb/^{204}Pb)_t$ vary from 18·17 to 18·88, with eight of the samples having ratios between 18·32 and 18·64. Moreover, most of the Pb isotope data define good positive correlations close to 150 Ma reference isochrons in plots of present-day $^{206}Pb/^{204}Pb$ vs $^{238}U/^{204}Pb$ and $^{208}Pb/^{204}Pb$ vs $^{232}Th/^{204}Pb$ (Fig. 9a,b), consistent with alteration largely occurring within a few million years after eruption for most of these samples. In both Fig. 4c and d, data for the 150 Ma rocks lie within the Pacific–North Atlantic MORB-source field, except for the leached split of sample MA-401, which falls slightly to the left of this field.

The 120 Ma alkalic lavas have lower $\varepsilon_{Nd}(t)$ than the 150 Ma rocks, from +6·0 to +2·9. Six of the ten samples show little variation in age-corrected $(^{206}Pb/^{204}Pb)_t$ ratios, which are between 18·81 and 19·00. In Fig. 4c, data points for these six samples plot toward the low-$\varepsilon_{Nd}(t)$ end of the Pacific–North Atlantic MORB-source array and in or near the Réunion–Crozet source field. In Fig. 4d, the data for these alkalic lavas lie beneath this field, and straddle the Pacific–North Atlantic MORB-source array. The remaining four samples analyzed have significantly lower $(^{206}Pb/^{204}Pb)_t$, between 18·49 and 17·71, yet have $\varepsilon_{Nd}(t)$ in exactly the same range as the other alkalic lavas. In Fig. 4d, the data point for one of these four samples falls well below the Pacific–North Atlantic MORB field, unlike any modern ridge or oceanic island basalts, and in Fig. 9c and d data for these samples lie far from the array defined by the others. We infer that relatively recent alteration (including variable loss of Pb) has seriously disturbed the Pb isotope systematics of these four alkalic lavas.

In addition to our work, Nägler & Frei (1997) have recently analyzed 120 Ma Masiran oceanic granites and amphibole-bearing gabbros, as well as several 150 Ma samples, for Nd and Pb isotopic ratios and U, Pb, Nd, and Sm abundances. Their age-corrected $\varepsilon_{Nd}(t)$ and $(^{206}Pb/^{204}Pb)_t$ values are similar to ours in that their data

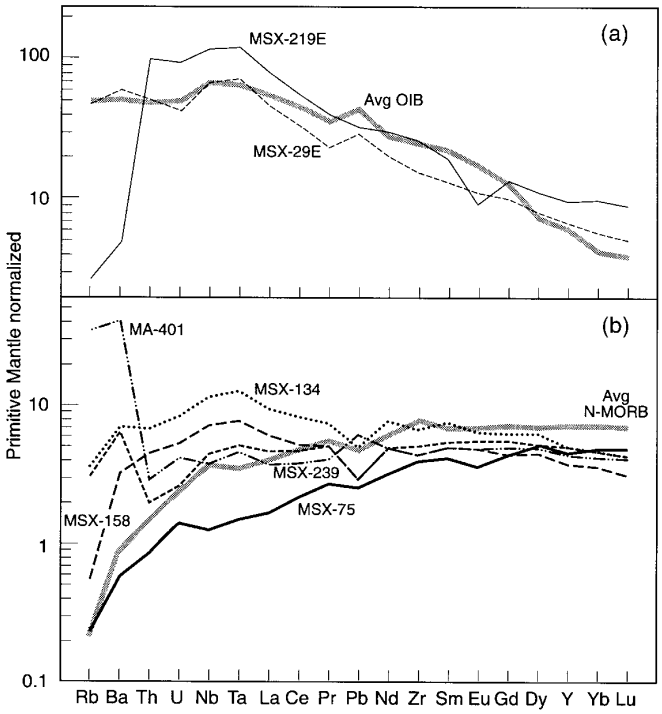

Fig. 8. Incompatible element patterns of selected Masirah 120 Ma alkalic lavas (a) and 150 Ma tholeiites (b).

fall largely within the estimated 150 Ma Pacific–North Atlantic MORB-source field of Fig. 4c or, for one granite, close to the Réunion–Crozet source field; also, as with our alkalic lavas, their 120 Ma gabbros and granites tend to have lower $\varepsilon_{Nd}(t)$ values than those of the 150 Ma rocks.

Yarlung–Zangpo suture zone

The samples from the Yarlung–Zangpo suture zone were collected from along the length of basalt outcrops to the southwest of Lhasa in the Xigaze area. Elemental and petrographic analyses of lavas from several of the same general areas show them to be chemically N-MORB (Pearce & Deng, 1988) altered to prehnite–pumpellyite or lower greenschist facies, with plagioclase replaced by albite and with abundant secondary groundmass actinolite and chlorite (Girardeau *et al.*, 1985). The lavas were erupted at an eastern Tethyan spreading center north of Greater Indo-Madagascar and to the south of the Tibetan block (see Fig. 7; Pozzi *et al.*, 1984). An age of 110 Ma was determined by Marcoux *et al.* (1982) from Radiolaria in cherts interbedded conformably with pillow basalts. Previous isotopic work on magmatic rocks consisted of Pb isotope and Pb and U (but not Th) abundance measurements by Göpel *et al.* (1984). Their results revealed a rough U–Pb whole-rock isochron (120 $\pm$ 10 Ma) which gave nearly the same age as the paleontologically derived age, indicating that the alteration affecting these rocks (including their U/Pb ratios) occurred fairly soon after eruption and that the rocks had remained nearly closed systems thereafter.

As with the Alexander Island basalts, Sr isotope ratios of the Yarlung–Zangpo samples are elevated relative to $\varepsilon_{Nd}(t)$, and acid-leaching yielded only modest reductions in $(^{87}Sr/^{86}Sr)_t$ (to 0·70380–0·70406; Fig. 3). These results are consistent with the similar level of alteration in the two suites, specifically with the extensive replacement of original plagioclase by albite (in the Yarlung–Zangpo basalts, clinopyroxene is also partly replaced with secondary phases). Values of $\varepsilon_{Nd}(t)$ show very little variation in the Yarlung–Zangpo samples, all being between +8·0 and +8·5, indicating a nearly homogeneous mantle source. The age-corrected Pb isotope ratios also vary only slightly: the spread in $(^{206}Pb/^{204}Pb)_t$, for example, is only 17·42–17·55 (in the same range as for Göpel *et al.*'s samples) and only 37·27–37·38 in $(^{208}Pb/^{204}Pb)_t$. Our results confirm the good overall positive correlation of present-day $^{206}Pb/^{204}Pb$ with $^{238}U/^{204}Pb$ as well. Most important for our present purposes, the Yarlung–Zangpo basalts define a very small field with a clear Indian-MORB-type signature in both Fig. 4c and d.

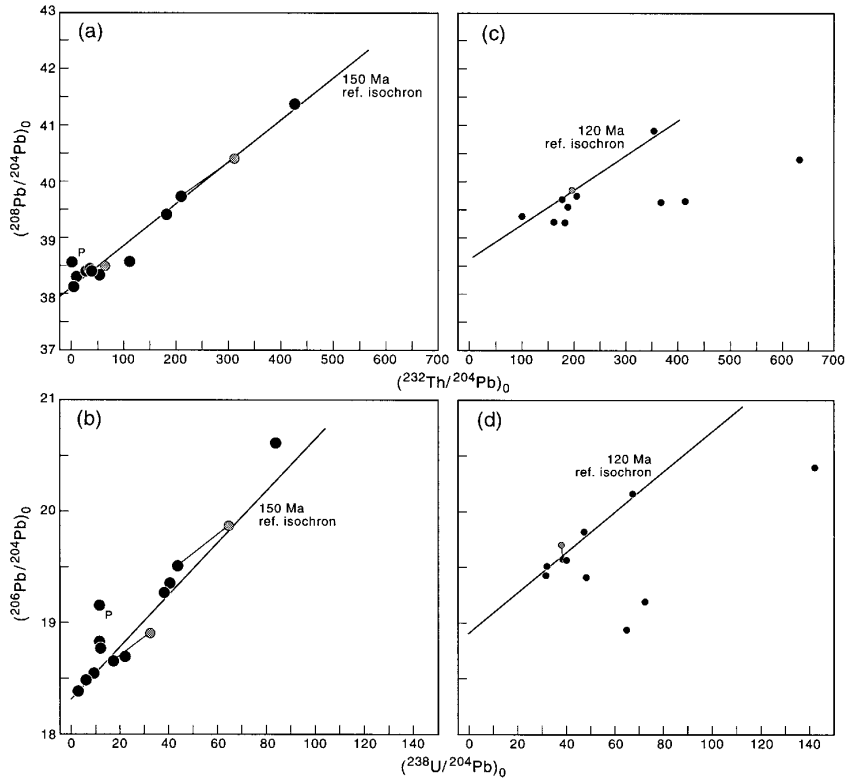

Fig. 9. Present-day $^{208}Pb/^{204}Pb$ vs $^{232}Th/^{204}Pb$ and $^{206}Pb/^{204}Pb$ vs $^{238}U/^{204}Pb$ for 150 Ma Masiran rocks (a, b) and for 120 Ma lavas (c, d); symbols as in Fig. 4. Also plotted are 150 Ma and 120 Ma reference isochrons. P is plagioclase separate.

DISCUSSION AND CONCLUSIONS

Consistent with the results for the Jurassic South Pacific lavas from Alexander Island, basalts of roughly similar age from several drill sites in the North Pacific recently have been shown to also possess Pacific–North-Atlantic-type age-adjusted isotopic signatures (Janney & Castillo, 1997). Allowing for relatively small changes in ε_{Nd} and Pb isotope ratios resulting from radiogenic ingrowth in the source mantle during the last 150 my, the available data thus imply that the Pacific MORB mantle in the Jurassic and earliest Cretaceous was isotopically very similar to that of today.

In the western Indian Ocean, the ~140 Ma Site 249 basalts reveal that Indian-Ocean-type isotopic compositions were present from almost the very beginning of the ocean itself—at least in some locations. However, the ~150 Ma rocks of Masirah and Site 261 (Weis & Frey, 1996) essentially lack normal Indian-MORB-type signatures. The crust at both sites formed near the southern boundary of the Tethyan Ocean, Masirah on the northwest and Site 261 on the northeast side of what would later become Greater India (see Fig. 7). Thus, the data for these sites provide no evidence that the Indian Ocean isotopic signature was inherited from Tethyan asthenosphere or, indeed, that the Indian Ocean mantle domain existed in anything like its present form north of East Gondwana in the Late Jurassic.

On the other hand, the Yarlung–Zangpo basalts demonstrate the existence of Indian-MORB-type mantle in at least a part of the equatorial Tethys by 110 Ma. In addition, some high-quality, age-corrected Pb and Nd isotopic data have been published for the Samail ophiolite of Oman, the crust of which appears to have formed at a low northern latitude (Perrin *et al.*, 1994) at ~95 Ma (e.g. Tilton *et al.*, 1981), to the west of that preserved in the Yarlung–Zangpo suture (see Fig. 7). In Fig. 4d, the Samail Pb isotope data occupy a restricted field above the Pacific–North Atlantic MORB-source array, and in Fig. 4c the combined Nd and Pb isotopic results [which were obtained on different samples (Chen & Pallister, 1981; McCulloch *et al.*, 1981)] define a rectangle that again largely falls outside the Pacific–North Atlantic MORB-source field (adjusted to a 95 Ma position; not shown in figure). Thus, the available data indicate an essentially Indian-Ocean-type mantle source for Samail crust at 95 Ma [see also Benoit (1997)].

Although very few locations have been studied as yet, the differences between the older and younger Tethyan

sites suggest the possibility of a temporal change in asthenospheric composition. A period of continental lithospheric thinning was followed by spreading in the eastern Indian Ocean at ~135 Ma (e.g. Powell *et al.*, 1988), and one possibility is that some Indian-MORB-type asthenosphere flowed northward out of the widening rift between Greater Indo-Madagascar and Australia–Antarctica, into parts of the Tethyan region. On the west side of Greater Indo-Madagascar, spreading and linkage with the Tethys began around 160–170 Ma (e.g. Lawver & Gahagan, 1993) (slightly before the 150 Ma Masiran rocks were formed), and northward flow of Indian-Ocean-type mantle may have begun earlier there. If so, to reach the paleolatitude of the Samail crust by 95 Ma, such asthenospheric flow must have occurred at rates of ~70–100 mm/yr; in comparison, rates of 25–40 mm/yr are indicated for westward flow of Pacific-type asthenosphere into the southeastern Indian Ocean between Antarctica and Australia since 43 Ma (Pyle *et al.*, 1992, 1995). Possible driving forces for significant asthenospheric outflow from the young, narrow Indian Ocean include (1) the ascent into the upper mantle of the large starting-plume heads of the Kerguelen, Marion, Bouvet, and Crozet hotspots [all of which may have reached the base of the lithosphere in the 200–120 Ma period; e.g. Storey (1995) and references therein], and (2) the upward advection of the 660 km boundary between upper and lower mantle proposed to have occurred beneath East Gondwana early in the Cretaceous in response to accelerated circum-Pacific subduction of slabs into the lower mantle (Larson & Kincaid, 1996). However, dispersion of stringers of Indian-Ocean-type mantle into the Tethys is not a unique explanation of the existing isotopic data. Although evidence is lacking for a widespread, pre-110 Ma Tethyan upper mantle possessing Indian-MORB-type characteristics, an alternative possibility is that the Tethyan asthenosphere may have contained pockets of both Pacific–North-Atlantic-type and Indian-MORB-type compositions (the latter presumably generated by the same types of processes as those acting in the Indian Ocean mantle) as far back as 150 Ma or even earlier. Study of Tethyan basalts from other locations along the southern Asian suture belt is required to evaluate these possibilities.

The 120 Ma alkalic lavas of Masirah have ocean-island-like elemental signatures, and six have isotopic compositions rather similar to those of modern Réunion (21°S) and Crozet (46°S) hotspot basalts, particularly in Fig. 4c. Recent plate reconstructions in the hotspot reference frame (e.g. Curray & Munasinghe, 1991; Lawver & Gahagan, 1993; Müller *et al.*, 1993) differ somewhat but suggest the Masiran region was situated between about 15°S and 25°S at 120 Ma, and thus appear to permit a Réunion connection of some sort (e.g. see Fig. 7) while ruling out an association with the Crozet hotspot, other than perhaps a 'far-field' effect related to dispersion of Crozet plume-head material. Meyer *et al.* (1996) recently suggested that the Marion (Prince Edward) hotspot, located to the west of Crozet, could have been the source of the alkalic magmatism; however, like Crozet, the Marion hotspot is located at ~46°S. Also, the volcanoes of the Marion hotspot have different isotopic compositions (e.g. $\varepsilon_{Nd} = +5{\cdot}7$ to $+7{\cdot}4$, $^{206}Pb/^{204}Pb = 18{\cdot}5$–$18{\cdot}6$; Hart, 1988; Mahoney *et al.*, 1992) from those of Réunion and Crozet. However, the origin of the 120 Ma Masiran rocks remains problematic, because although the isotopic signature of the main component in the Réunion plume appears to have changed little in the last 66 my (White *et al.*, 1990; Peng & Mahoney, 1995), the Réunion hotspot is believed by most workers to have appeared only shortly before 66 Ma, the Deccan Traps event being interpreted as the hotspot's initial, plume-head phase [e.g. Basu *et al.* (1993) and references therein].

Both Indian-Ocean-type and some Pacific–North-Atlantic-type isotopic signatures are preserved in the old western Indian Ocean drill sites. Moreover, when results for the drillholes are combined with those for Afanasy-Nikitin Seamount, a 3 ε_{Nd} unit wider total spread of $\varepsilon_{Nd}(t)$ is encompassed than is found for present-day Indian MORB and oceanic islands (compare Figs 1a and 4a). This comparison excludes the Early Cretaceous Kerguelen and Naturaliste plateaux, which reach even lower $\varepsilon_{Nd}(t)$ values than Afanasy-Nikitin but, unlike Afanasy-Nikitin, probably contain blocks of continental lithosphere [e.g. see Mahoney *et al.* (1996) and references therein]; it also excludes recent lavas (with less extreme values; e.g. Weis *et al.*, 1992) erupted through the thick lithosphere of the Kerguelen Plateau. As such, the total range in $\varepsilon_{Nd}(t)$ for modern (0–10 Ma) Indian Ocean basalts is $-4{\cdot}0$ to $+11{\cdot}3$, whereas that for the old lavas is $-8{\cdot}0$ to $+10{\cdot}3$, with both maximum and minimum values seen in lavas formed at 60–80 Ma (note that Site 261 in the northeastern Indian Ocean, although formed at a Tethyan ridge, yielded an even higher value of $+14{\cdot}4$; Weis & Frey, 1996). This difference is much greater than achievable by plausible isotopic evolution (i.e. 'aging') in the source mantle since the Cretaceous.

The larger isotopic range observed for the old basalts is remarkable in view of the very sparse sampling of old Indian Ocean crust relative to sampling of the present-day spreading centers and islands; further, it is unlikely that the few existing old sites have fortuitously sampled the full isotopic range present in old Indian Ocean seafloor. Admittedly, substantial sections of the modern spreading system remain unsampled or have only recently been dredged, and could potentially harbor more extreme isotopic compositions than found elsewhere. However, continuing work on the largest previously unsampled stretch of the system, the Southeast Indian Ridge between

the Australian–Antarctic Discordance and St Paul Island, thus far reveals isotopic values that are all well within the previous range for modern Indian MORB (Hall *et al.*, 1995; unpublished data, 1997). Nor does it appear that the difference in isotopic ranges can be ascribed in any simple way to differences in spreading rate. Greater isotopic heterogeneity along ridges generally is associated with slower spreading rates—for example, both the highest and lowest ε_{Nd} values observed in the modern Indian Ocean (+11·3 and –4·0) are found on the central part of the very slowly spreading Southwest Indian Ridge (Mahoney *et al.*, 1992). However, the old Indian Ocean samples with both the highest and lowest ε_{Nd} values were formed (also on-ridge or very near-ridge) in the 60–80 Ma period of super-fast spreading (e.g. Fisher & Sclater, 1983). The most straightforward interpretation of the existing data is therefore that the Indian Ocean asthenosphere was isotopically more heterogeneous in the past and is gradually becoming better mixed on a time scale of tens of millions of years. In turn, greater heterogeneity in the not too distant past, including the presence in some locations of Pacific–North-Atlantic-type compositions, is most consistent with a relatively young origin for the Indian Ocean mantle domain; that is, one not considerably older than the age of the Indian Ocean itself.

ACKNOWLEDGEMENTS

Reviews by R. Hickey-Vargas, P. Janney, and D. Pyle are gratefully acknowledged, as are helpful informal comments by P. Castillo and F. Frey. We thank F. Moseley, T.-Y. Guo, and the Ocean Drilling Program for providing samples, and N. Hulbirt, Z. Peng, K. Spencer, and D. VonderHaar for help with various aspects of the work. This work was funded by NSF grant EAR94-18168.

REFERENCES

Abbotts, I. L. (1981). Masirah (Oman) ophiolite sheeted dykes and pillow lavas: geochemical evidence of the former ocean ridge environment. *Lithos* **14,** 283–294.

Bach, W., Hegner, E., Erzinger, J. & Satir, M. (1994). Chemical and isotopic variations along the superfast spreading East Pacific Rise from 6° to 30°S. *Contributions to Mineralogy and Petrology* **116,** 365–380.

Barker, P. F., Kennett, J. P. *et al.* (1990). *Proceedings of the Ocean Drilling Program, Scientific Results* **113.** Washington, DC: US Government Printing Office.

Basu, A. R., Renne, P. R., DasGupta, D. K., Teichmann, F. & Poreda, R. J. (1993). Early and late alkali igneous pulses and a high-^{3}He plume origin for the Deccan flood basalts. *Science* **261,** 902–906.

Benoit, M. (1977). Caractérisation géochimique (traces, isotopes) d'un système de drainage magmatique fossile dans l'ophiolite d'Oman. Ph.D. Thesis, Université Paul Sabatier, Toulouse, 166 pp.

Bienvenu, P., Bougault, H., Joron, M. & Dmitriev, L. (1990). MORB alteration: rare-earth element/non-rare-earth hygromagmaphile element fractionation. *Chemical Geology* **82,** 1–14.

Castillo, P. R. (1988). The Dupal anomaly as a trace of the upwelling lower mantle. *Nature* **336,** 667–670.

Castillo, P. R. (1996). Origin and geodynamic implication of the Dupal isotopic anomaly in volcanic rocks from the Philippine island arcs. *Geology* **24,** 271–274.

Chen, J. H. & Pallister, J. S. (1981). Lead isotopic studies of the Samail ophiolite, Oman. *Journal of Geophysical Research* **86,** 2699–2708.

Coleman, R. G. (1981). Tectonic setting for ophiolite obduction in Oman. *Journal of Geophysical Research* **86,** 2497–2508.

Crawford, A. J., Briqueu, L., Laporte, C. & Hasenaka, T. (1995). Coexistence of Indian and Pacific oceanic upper mantle reservoirs beneath the central New Hebrides island arc. In: Taylor, B. & Natland, J. H. (eds) *Active Margins and Marginal Basins of the Western Pacific. Geophysical Monograph, American Geophysical Union* **88,** 199–217.

Curray, J. R. & Munasinghe, T. (1991). Origin of the Rajmahal Traps and 85°E Ridge: preliminary reconstructions of the trace of the Crozet hotspot. *Geology* **19,** 1237–1240.

Davies, T. A., Luyendyk, B. P. *et al.* (1994). *Initial Reports of the Deep Sea Drilling Project* **26.** Washington, DC: US Government Printing Office, 1129 pp.

Dosso, L., Bougault, H., Beuzart, P., Calvez, J.-Y. & Joron, J.-L. (1988). The geochemical structure of the South-East Indian Ridge. *Earth and Planetary Science Letters* **88,** 47–59.

Dosso, L., Bougault, H. & Joron, J.-L. (1993). Geochemical morphology of the north Mid-Atlantic Ridge, 10°–24°N: trace element-isotope complementarity. *Earth and Planetary Science Letters* **120,** 443–462.

Doubleday, P. A., Leat, P. T., Alabaster, T., Nell, P. A. R. & Tranter, T. H. (1994). Allochthonous oceanic basalts within the Mesozoic accretionary complex of Alexander Island, Antarctica: remnants of proto-Pacific oceanic crust. *Journal of the Geological Society, London* **151,** 65–78.

Dupré, B. & Allègre, C. J. (1983). Pb–Sr isotope variations in Indian Ocean basalts and mixing phenomena. *Nature* **303,** 142–146.

Fisher, R. L. & Sclater, J. G. (1983). Tectonic evolution of the Southwest Indian Ocean since the Mid-Cretaceous: plate motions and stability of the pole of Antarctica/Africa for at least 80 Myr. *Geophysical Journal of the Royal Astronomical Society* **73,** 553–576.

Fisher, R. L., Bunce, E. T. *et al.* (1974). *Initial Reports of the Deep Sea Drilling Project* **24.** Washington, DC: US Government Printing Office, 1183 pp.

Fisher, R. L., Dick, H. J. B., Natland, J. H. & Meyer, P. S. (1986). Mafic/ultramafic suites of the slowly spreading Southwest Indian Ridge: Protea exploration of the Antarctic plate boundary, 24°–47°E, (1984). *Ofioliti* **11,** 147–178.

Girardeau, J., Mercier, J.-C. C. & Wang, X. B. (1985). Petrology of the mafic rocks of the Xigaze ophiolite, Tibet. *Contributions to Mineralogy and Petrology* **90,** 309–321.

Gnos, E. & Perrin, M. (1996). Formation and evolution of the Masirah ophiolite constrained by paleomagnetic study of volcanic rocks. *Tectonophysics* **253,** 53–64.

Göpel, C., Allègre, C. J. & Xu, R.-H. (1984). Lead isotopic study of the Xigaze ophiolite (Tibet): the problem of the relationship between magmatites (gabbros, dolerites, lavas) and tectonites (harzburgites). *Earth and Planetary Science Letters* **69,** 301–310.

Govindaraju, K. (1989). Compilation of working values and sample descriptions for 272 geostandards. *Geostandards Newsletter* **13,** 1–113.

Hall, L. S., Mahoney, J. J. & Christie, D. M. (1995). First Nd, Sr, and Pb isotope analyses for the Southeast Indian Ridge 88°–118°E. *Eos Transactions, American Geophysical Union* **76,** F259–260.

Hamelin, B., Dupré, B. & Allègre, C. J. (1986). Pb–Sr–Nd isotopic data of Indian Ocean ridges: new evidence of large-scale mapping of mantle heterogeneities. *Earth and Planetary Science Letters* **76,** 288–298.

Hanan, B. B. & Schilling, J.-G. (1989). Easter Microplate evolution: Pb isotope evidence. *Journal of Geophysical Research* **94,** 7432–7448.

Hart, S. R. (1984). A large-scale isotope anomaly in the Southern Hemisphere mantle. *Nature* **309,** 753–757.

Hart, S. R. (1988). Heterogeneous mantle domains: signatures, genesis and mixing chronologies. *Earth and Planetary Science Letters* **90,** 273–296.

Hedge, C. E., Futa, K., Engel, C. G. & Fisher, R. L. (1979). Rare earth abundances and Rb–Sr systematics of basalts, gabbro, anorthosite and minor granitic rocks from the Indian Ocean ridge system, western Indian Ocean. *Contributions to Mineralogy and Petrology* **68,** 373–376.

Hickey-Vargas, R. (1991). Isotope characteristics of submarine lavas from the Philippine tectonic plate. *Earth and Planetary Science Letters* **107,** 290–304.

Hickey-Vargas, R. (1998). Origin of the Indian-Ocean-type signature in basalts from Philippine Sea Plate spreading centers: an assessment of local versus large-scale processes. *Journal of Geophysical Research* (in press).

Hickey-Vargas, R., Hergt, J. M. & Spadea, P. (1995). The Indian Ocean-type isotopic signature in Western Pacific marginal basins: origin and significance. In: Taylor, B. & Natland, J. H. (eds) *Active Margins and Marginal Basins of the Western Pacific. Geophysical Monograph, American Geophysical Union* **88,** 175–197.

Hochstaedter, A. G., Gill, J. B. & Morris, J. D. (1990). Volcanism in the Sumisu Rift II: subduction and non-subduction related components. *Earth and Planetary Science Letters* **100,** 195–209.

Immenhauser, A. (1996). Cretaceous sedimentary rocks of the Masirah ophiolite (Sultanate of Oman): evidence for an unusual bathymetric history. *Journal of the Geological Society, London* **153,** 539–551.

Ito, E., White, W. M. & Göpel, C. (1987). The O, Sr, Nd, and Pb isotope geochemistry of MORB. *Chemical Geology* **62,** 157–176.

Jain, J. C. & Neal, C. R. (1996). Report of the ICP-MS facility, 1993–1996. Notre Dame University Open File Report, 30 pp.

Janney, P. E. & Castillo, P. R. (1997). Geochemistry of Mesozoic Pacific MORB: constraints on melt generation and the evolution of the Pacific upper mantle. *Journal of Geophysical Research* **102,** 5207–5229.

Jochum, K. P. & Verma, S. P. (1996). Extreme enrichment of Sb, Tl and other trace elements in altered MORB. *Chemical Geology* **130,** 289–299.

Klein, E. M., Langmuir, C. H., Zindler, A., Staudigel, H. & Hamelin, B. (1988). Isotope evidence of a mantle convection boundary at the Australian–Antarctic Discordance. *Nature* **297,** 43–46.

Lanyon, R. (1995). The Balleny plume, the Australian–Antarctic Discordance, and U–Pb zircon dating of an Antarctic mafic dyke swarm. Ph.D. Thesis, University of Tasmania, Hobart, 407 pp.

Larson, R. L. & Kincaid, C. (1996). Onset of Mid-Cretaceous volcanism by elevation of the 670 km thermal boundary layer. *Geology* **24,** 551–554.

Lawver, L. A. & Gahagan, L. M. (1993). Subduction zones, magmatism, and the breakup of Pangea. In: Stone, D. B. & Runcorn, S. K. (eds) *Flow and Creep in the Solar System: Observations, Modeling and Theory*. Dordrecht: Kluwer Academic, pp. 225–247.

le Roex, A. P., Dick, H. J. B. & Fisher, R. L. (1989). Petrology and geochemistry of MORB from 25°E to 46°E along the Southwest Indian Ridge: evidence for contrasting styles of mantle enrichment. *Journal of Petrology* **30,** 947–986.

Li, Y.-H. (1991). Distribution patterns of elements in the ocean: a synthesis. *Geochimica et Cosmochimica Acta* **55,** 3224–3252.

Loock, G., McDonough, W. F., Goldstein, S. L. & Hofmann, A. W. (1990). Isotopic compositions of volcanic glasses from the Lau Basin. *Marine Mining* **9,** 235–245.

Macdougall, J. D., Finkel, R. C., Carlson, J. & Krishnaswami, S. (1979). Isotopic evidence for uranium exchange during low-temperature alteration of oceanic basalt. *Earth and Planetary Science Letters* **42,** 27–34.

Mahoney, J. J. (1987). An isotopic survey of Pacific oceanic plateaus: implications for their nature and origin. In: Keating, B. H., Fryer, P., Batiza, R. & Boehlert, G. W. (eds) *Seamounts, Islands, and Atolls. Geophysical Monograph, American Geophysical Union* **43,** 207–220.

Mahoney, J. J. & Spencer, K. J. (1991). Isotopic evidence for the origin of the Manihiki and Ontong Java oceanic plateaus. *Earth and Planetary Science Letters* **104,** 196–210.

Mahoney, J. J., Natland, J. H., White, W. M., Poreda, R., Bloomer, S. H., Fisher, R. L. & Baxter, A. N. (1989). Isotopic and geochemical provinces of the western Indian Ocean spreading centers. *Journal of Geophysical Research* **94,** 4033–4053.

Mahoney, J., le Roex, A. P., Peng, Z., Fisher, R. L. & Natland, J. H. (1992). Southwestern limits of Indian Ocean ridge mantle and the origin of low $^{206}Pb/^{204}Pb$ mid-ocean ridge basalt: isotope systematics of the central Southwest Indian Ridge (17°–50°E). *Journal of Geophysical Research* **97,** 19771–19790.

Mahoney, J. J., Sinton, J. M., Kurz, M. D., Macdougall, J. D., Spencer, K. J. & Lugmair, G. W. (1994). Isotope and trace element characteristics of a super-fast spreading ridge: East Pacific Rise, 13–23°S. *Earth and Planetary Science Letters* **121,** 173–193.

Mahoney, J. J., White, W. M., Upton, B. G. J., Neal, C. R. & Scrutton, R. A. (1996). Beyond EM-1: lavas from Afanasy-Nikitin Rise and the Crozet Archipelago, Indian Ocean. *Geology* **24,** 615–618.

Marcoux, J., De Wever, P., Nicolas, A., Girardeau, J., Xiao, X., Chang, C., Wang, N., Zao, Y., Bassoullet, J. P., Colchen, M. & Mascle, G. (1982). Preliminary report on depositional sediments on top of the volcanic member: the Xigaze ophiolite (Yarlung–Zangpo suture zone). *Ofioliti* **2–3,** 395–396.

McCulloch, M. T., Gregory, R. T., Wasserburg, G. J. & Taylor, H. T. (1981). Sm–Nd, Rb–Sr, and $^{18}O/^{16}O$ isotope systematics in an oceanic crustal section: evidence from the Samail ophiolite. *Journal of Geophysical Research* **86,** 2721–2735.

Meyer, J., Mercoulli, I. & Immenhauser, A. (1996). Off-ridge alkaline magmatism and seamount volcanoes in the Masirah Island ophiolite, Oman. *Tectonophysics* **267,** 187–208.

Michard, A., Montigny, R. & Schlich, R. (1986). Geochemistry of the mantle beneath the Rodrigues triple junction and the South-East Indian Ridge. *Earth and Planetary Science Letters* **78,** 104–114.

Moseley, F. (1990). The structure of Masirah Island, Oman. In: Robertson, A., Searle, M. & Ries, A. (eds) *The Geology and Tectonics of the Oman Region. Special Publication, Geological Society, London* **49,** 665–671.

Moseley, F. & Abbotts, I. L. (1979). The ophiolite mélange of Masirah, Oman. *Journal of the Geological Society, London* **136,** 713–724.

Mountain, G. S. & Prell, W. L. (1990). A multiphase plate-tectonic history of the southeast continental margin of Oman. In: Robertson, A., Searle, M. & Ries, A. (eds) *The Geology and Tectonics of the Oman Region. Special Publication, Geological Society, London* **49,** 725–743.

Mukasa, S. B., McCabe, R. & Gill, J. B. (1987). Pb isotopic compositions of volcanic rocks in the west and east Philippine island arcs: presence of the Dupal isotopic anomaly. *Earth and Planetary Science Letters* **84,** 153–164.

Müller, R. D., Royer, J.-Y. & Lawver, L. A. (1993). Revised plate motions relative to the hotspots from combined Atlantic and Indian Ocean hotspot tracks. *Geology* **21,** 275–278.

Nägler, T. & Frei, R. (1997). True K-feldspar granites in oceanic crust (Masirah ophiolite, Sultanate of Oman): a U–Pb and Sm–Nd isotopic study. *Chemical Geology* **138,** 119–126.

Ogg, J. G., Kodama, K. & Wallick, B. P. (1992). Lower Cretaceous magnetostratigraphy and paleolatitudes off northwestern Australia, ODP Site 765 and DSDP Site 261, Argo Abyssal Plain, and ODP Site 766, Gascoyne Abyssal Plain. *Proceedings of the Ocean Drilling Program, Scientific Results,* **123.** College Station, TX: Ocean Drilling Program, pp. 523–547.

Pearce, J. A. & Deng, W. (1988). The ophiolites of the Tibetan geotraverses, Lhasa to Golmud (1985) and Lhasa to Kathmandu (1986). *Philosophical Transactions of the Royal Society of London, Series A* **327,** 215–238.

Peng, Z. X. & Mahoney, J. J. (1995). Drillhole lavas from the northwestern Deccan Traps and the evolution of Réunion hotspot mantle. *Earth and Planetary Science Letters* **134,** 169–185.

Perrin, M., Prevot, M. & Bruere, F. (1994). Rotation of the Oman ophiolite and initial location of the ridge in the hotspot reference frame. *Tectonophysics* **229,** 31–42.

Powell, C. M., Roots, S. R. & Veevers, J. (1988). Pre-breakup continental extension in east Gondwana and the early opening of the eastern Indian Ocean. *Tectonophysics* **155,** 261–283.

Pozzi, J. P., Westphal, M., Girardeau, J., Besse, J. & Zhou, Y. X. (1984). Paleomagnetism of the Xigaze ophiolite and flysch: latitude and direction of spreading. *Earth and Planetary Science Letters* **70,** 383–394.

Price, R. C., Kennedy, A. K., Riggs-Sneeringer, M. & Frey, F. A. (1986). Geochemistry of basalts from the Indian Ocean triple junction: implications for the generation and evolution of Indian Ocean ridge basalts. *Earth and Planetary Science Letters* **78,** 379–396.

Pyle, D. G., Christie, D. M. & Mahoney, J. J. (1992). Resolving an isotopic boundary within the Australian–Antarctic Discordance. *Earth and Planetary Science Letters* **112,** 161–178.

Pyle, D. G., Christie, D. M., Mahoney, J. J. & Duncan, R. A. (1995). Geochemistry and geochronology of ancient southeast Indian and southwest Pacific seafloor. *Journal of Geophysical Research* **100,** 22261–22282.

Rehkämper, M. & Hofmann, A. W. (1997). Recycled ocean crust and sediment in Indian Ocean MORB. *Earth and Planetary Science Letters* **147,** 93–l06.

Schandl, E. S., Gorton, M. P. & Wicks, F. J. (1990). Mineralogy and geochemistry of alkali basalts from Maud Rise, Weddell Sea, Antarctica. *Proceedings of the Ocean Drilling Program, Scientific Results,* **113.** College Station, TX: Ocean Drilling Program, pp. 5–11.

Schilling, J.-G., Kingsley, R. H., Hanan, B. B. & McCully, B. L. (1992). Nd–Sr–Pb isotopic variations along the Gulf of Aden: evidence for Afar mantle plume–continental lithosphere interaction. *Journal of Geophysical Research* **97,** 10927–10966.

Simpson, E. S. W., Schlich, R. *et al.* (1974). *Initial Reports of the Deep Sea Drilling Project,* **25.** Washington, DC: US Government Printing Office, 884 pp.

Smewing, J. D., Abbotts, I. L., Dunne, L. A. & Rex, D. C. (1991). Formation and emplacement ages of the Masirah ophiolite, Sultanate of Oman. *Geology* **19,** 453–456.

Spadea, P., D'Antonio, M. & Thirlwall, M. F. (1996). Source characteristics of basement rocks from the Sulu and Celebes basins (Western Pacific): chemical and isotopic evidence. *Contributions to Mineralogy and Petrology* **123,** 159–176.

Staudigel, H., Muehlenbachs, K., Richardson, S. H. & Hart, S. R. (1981). Agents of low-temperature ocean crust alteration. *Contributions to Mineralogy and Petrology* **77,** 150–157.

Staudigel, H., Davies, G. R., Hart, S. R., Marchant, K. M. & Smith, B. M. (1995). Large scale Sr, Nd and O isotopic anatomy of altered oceanic crust: DSDP/ODP sites 417/418. *Earth and Planetary Science Letters* **130,** 169–185.

Storey, B. C. (1995). The role of mantle plumes in continental breakup: case histories from Gondwanaland. *Nature* **377,** 301–308.

Storey, M., Saunders, A. D., Tarney, J., Gibson, I. L., Norry, M. J., Thirlwall, M. F., Leat, P., Thompson, R. N. & Menzies, M. A. (1989). Contamination of Indian Ocean asthenosphere by the Kerguelen–Heard mantle plume. *Nature* **338,** 574–576.

Storey, M., Kent, R., Saunders, A. D., Salters, V. J., Hergt, J., Whitechurch, H., Sevigny, J. H., Thirlwall, M. F., Leat, P., Ghose, N. C. & Gifford, M. (1992). Lower Cretaceous volcanic rocks along continental margins and their relationship to the Kerguelen Plateau. *Proceedings of the Ocean Drilling Program, Scientific Results,* **120.** College Station, TX: Ocean Drilling Program, pp. 33–54.

Sun, S.-S. (1980). Lead isotopic study of young volcanic rocks from mid-ocean ridges, ocean islands and island arcs. *Philosophical Transactions of the Royal Society of London, Series A* **297,** 409–445.

Sun, S.-S. & McDonough, W. F. (1989). Chemical and isotopic systematics of oceanic basalts: implications for mantle composition and processes. In: Saunders, A. D. & Norry, M. J. (eds) *Magmatism in the Ocean Basins. Special Publication, Geological Society, London* **42,** 313–345.

Tatsumoto, M. (1978). Isotopic composition of lead in oceanic basalt and its implication to mantle evolution. *Earth and Planetary Science Letters* **38,** 63–87.

Tilton, G. R., Hopson, C. A. & Wright, J. E. (1981). Uranium–lead isotopic ages of the Samail ophiolite, Oman, with applications to Tethyan Ocean ridge tectonics. *Journal of Geophysical Research* **86,** 2763–2775.

Todt, W., Cliff, R. A., Hanser, A. & Hofmann, A. W. (1996). Evaluation of a ^{202}Pb–^{205}Pb double spike for high-precision lead isotopic analyses. In: Basu, A. & Hart, S. (eds) *Earth Processes, Reading the Isotopic Code. Geophysical Monograph, American Geophysical Union* **95,** 429–437.

Tu, K., Flower, M. F., Carlson, R. W., Xie, G., Chen, C.-Y. & Zhang, M. (1992). Magmatism in the South China Basin. 1. Isotopic and trace-element evidence for an endogenous Dupal mantle component. *Chemical Geology* **97,** 47–63.

Volker, F., McCulloch, M. & Altherr, R. (1993). Submarine basalts from the Red Sea: new Pb, Sr, and Nd isotopic data. *Geophysical Research Letters* **20,** 927–930.

Weis, D. & Frey, F. A. (1996). Role of the Kerguelen plume in generating the eastern Indian Ocean seafloor. *Journal of Geophysical Research* **101,** 13841–13849.

Weis, D., White, W. M., Frey, F. A., Duncan, R. A., Dehn, J., Fisk, M., Ludden, J., Saunders, A. & Storey, M. (1992). The influence of mantle plumes in generation of Indian Ocean crust. In: Duncan, R. A., Rea, D. K., Kidd, R. B., von Rad, U. & Weissel, J. J. (eds) *Synthesis of Results from Scientific Drilling in the Indian Ocean. Geophysical Monograph, American Geophysical Union* **70,** 57–89.

White, W. M. (1993). $^{238}U/^{204}Pb$ in MORB and open system evolution of the depleted mantle. *Earth and Planetary Science Letters* **115,** 211–226.

White, W. M., Hofmann, A. W. & Puchelt, H. (1987). Isotope geochemistry of Pacific mid-ocean ridge basalt. *Journal of Geophysical Research* **92,** 4881–4893.

White, W. M., Cheatham, M. M. & Duncan, R. A. (1990). Isotope geochemistry of Leg 115 basalts and inferences on the history of the Réunion mantle plume. *Proceedings of the Ocean Drilling Program, Scientific Results,* **115.** College Station, TX: Ocean Drilling Program, pp. 53–62.

Whitmarsh, R. B., Weser, O. E. *et al.* (1974). *Initial Reports of the Deep Sea Drilling Project,* **23.** Washington, DC: US Government Printing Office, 1180 pp.